Histone methylation regulates reproductive diapause in *Drosophila melanogaster*

Abigail DiVito Evans[1,2], Regina A. Fairbanks[1,2], Paul Schmidt[1], Mia T. Levine[1,2]*

[1]Department of Biology, School of Arts and Sciences, University of Pennsylvania, Philadelphia, PA
[2]Epigenetics Institute, University of Pennsylvania, Philadelphia, PA

Keywords: diapause, developmental plasticity, epigenetics, chromatin, *Drosophila*

*Lead contact:

Mia Levine, University of Pennsylvania, 433 S. University Avenue, Philadelphia, PA 19104. p: 215-573-9709 e: m.levine@sas.upenn.edu.

ABSTRACT

Fluctuating environments pose distinct threats to developing organisms. To better match the immediate, local environment, many organisms adopt alternative developmental fates. The mechanism by which an individual, subjected to a suboptimal environment, exercises this “developmental plasticity” is poorly understood. Here we test the hypothesis that environment-dependent developmental plasticity is mediated by epigenetic factors. To model developmental plasticity, we exploit the reversible reproductive arrest of *Drosophila melanogaster* females called diapause. Using an inbred line, we demonstrate that diapause plasticity is epigenetic: only a subset of genetically identical individuals enter diapause, and this state of reproductive arrest is epigenetically transmitted for at least three generations. Furthermore, we show that active chromatin marks H3K4me3 and H3K36me1 are depleted in diapausing ovaries. Using ovary-specific RNAi against histone mark writers and erasers, we demonstrate that H3K4me3 and H3K36me1 depletion promotes diapause plasticity. Surprisingly, while H3K4me3 and H3K36me1 determine diapause plasticity in an inbred line with high plasticity, these two marks are similarly abundant across the diapausing and reproductive ovaries of a genotypically distinct inbred line with low plasticity. These data suggest genetic variation for epigenetic regulation of reproductive diapause. Consistent with this possibility, the diapause-specific gene expression program also varies across the two genotypes. These data reveal new chromatin determinants of diapause plasticity and suggest that these determinants may be genotype-dependent. This study provides new insight into how organisms exploit epigenetic mechanisms to persist in fluctuating environments.

INTRODUCTION

Alternative environmental conditions can give rise to alternative developmental trajectories. This "developmental plasticity" enables a better match between an individual's local environment and its phenotype. For example, seasonal snow cover triggers a coat color change from brown to white in the boreal snowshoe hare. Once the snow cover melts, the hare redevelops a brown coat (1). Similarly, limited resource availability triggers *C. elegans* juveniles to enter physiological arrest. Once resource availability improves, the juveniles resume development into adults (2, 3). Developmental plasticity is ubiquitous across multicellular organisms (4); however, the mechanisms by which the same genotype – in response to distinct environments – gives rise to distinct developmental fates are poorly understood (4-8).

While the regulatory mechanisms of environment-sensitive developmental fate plasticity are largely unknown, the regulatory mechanisms of cell fate plasticity are well-established. Epigenetic mechanisms such as DNA packaging into alternative chromatin states determines distinct gene expression programs and, ultimately, distinct cellular identities [(9-12) reviewed in (13-15)]. These alternative chromatin states include differential chemical modifications to either the DNA or the histone proteins that make up the nucleosome around which DNA wraps. The addition and removal of acetyl and methyl groups from histone tails can alter the transcriptional state of chromatin and promote distinct cell fates in response to intrinsic developmental cues [(16, 17), reviewed in (18, 19)]. Intriguingly, extrinsic environmental cues can also alter DNA packaging into chromatin (20-26). Drought, temperature, salinity, and exposure to toxins alter the genome-wide distribution and abundance of acetyl and methyl groups on histone tails [reviewed in (27, 28)]. The observation that chromatin packaging is both environment-sensitive and a key determinant of cell fate during development raises the possibility that chromatin may mediate environment-sensitive developmental plasticity (29).

Consistent with this possibility, a handful of studies have established causal links between chromatin and developmental plasticity (29-34). Three of these studies probe chromatin-based regulation of developmental arrest. To escape unfavorable environmental conditions, some organisms enter a state of dormancy such that development is suspended and senescence is slowed. Dormancy can occur at any developmental stage, from embryo to adult. In juvenile dormancy, a paused transition between developmental stages results in dramatic lifespan extensions. In adult dormancy, both somatic lifespan and reproductive lifespan are extended. While several groundbreaking studies have identified chromatin-based regulation of juvenile dormancy (31, 33, 34), the chromatin determinants of adult dormancy, and specifically the preservation of reproductive potential at this life stage, have not yet been explored.

To investigate chromatin-based regulation of reproductive preservation in dormancy, we exploit the tractable model system, *Drosophila melanogaster. D. melanogaster* enters a form of adult dormancy called diapause in response to the cold temperatures and short days of oncoming winter [as defined in (35-38), but see (39)]. *Drosophila* diapause in females is characterized by extensive physiological changes that result in increased lipid storage, increased stress tolerance, suspended egg production, and lifespan extension (40-44). Remarkably, *D. melanogaster* females retain nearly full reproductive potential following diapause (37, 42, 45, 46). Here we report that *D. melanogaster* reproductive diapause is epigenetically regulated. We found two histone modifications that regulate reproductive diapause through a mechanism distinct from those previously identified in juvenile diapause (31, 33, 34). We also report that the diapause-associated depletion of these two histone marks is genotype-dependent, suggesting diverged chromatin-based regulation of diapause between genotypes within a species. These data provide new insight into how organisms exploit epigenetic mechanisms to persist in fluctuating environments.

RESULTS

Establishing a system to study epigenetic regulation of reproductive plasticity

To study the chromatin determinants of reproductive lifespan extension under diapause, we established a system wherein epigenetic regulation, including chromatin-based regulation, could be isolated from the often-confounding effects of genotype, environment, and tissue heterogeneity. *D. melanogaster* diapause emerged as a compelling candidate system. This system allows us to control for genetic variation, evaluate alternative developmental fates in the same environment, and microdissect ovaries to ensure tissue homogeneity across alternative developmental fates.

To control for genotypic effects on epigenetics, we inbred an isofemale line from a temperate North American population (collected in Pennsylvania) by brother-sister mating for 10 generations. Under simulated winter conditions (Fig. 1A), 87.9% of inbred females enter diapause (Fig. 1B), an incidence typical of isofemale lines from the same region (43). This incomplete diapause penetrance, where most females arrest but some (12.1%) remain persistently reproductive upon exposure to simulated winter conditions, allows us to control for environment in addition to genotype: we can compare the chromatin state of inbred diapause and persistently reproductive individuals in the same environment. Finally, to control for tissue heterogeneity, we isolated only those ovary stages represented in diapause (stages 1-7, see Fig. 1B) in all experiments that compare arrested and reproductive ovaries.

This discovery of environment-induced alternative developmental fates across individuals of a single genotype implicates epigenetic regulation. Another hallmark of epigenetic regulation is transgenerational transmission of parental environmental conditions to offspring (47-50). To probe the possibility that the parental diapause environment is transmitted to offspring, we assayed diapause plasticity of daughters, granddaughters, and great-granddaughters of inbred females that had undergone diapause (Fig. 1C). We first subjected a cohort of females to winter conditions (12°C, Fig. 1C “naïve females”). We allowed the subset of females that had entered diapause to mate and reproduce at 25°C. We assayed one cohort of their daughters for diapause plasticity (Fig. 1C “daughters”, one generation since diapause) and allowed a second cohort to mate and reproduce at 25°C. We repeated this process until the great-granddaughter generation (Fig. 1C “great granddaughters”, three generations since diapause). These experiments revealed that diapause entry in mothers reduces diapause plasticity (the percent of females with arrested ovaries) in daughters ($p<2.2x10^{-16}$), granddaughters ($p<2.2x10^{-16}$), and great-granddaughters ($p=4.6x10^{-8}$), Fig. 1D). Moreover, this transgenerational effect decreases with each generation removed from the initial incidence of diapause. The dilution of the transgenerational effect suggests dilution of an epigenetic signal through generations [(51), reviewed in (52)]. Such transgenerational effects further implicate a role for epigenetic regulation of diapause plasticity.

A classic readout of epigenetically regulated, alternative developmental fates is alternative gene expression programs across genetically identical individuals (53). To profile gene expression across the two developmental fates, we performed RNA-seq on both arrested and persistently reproductive ovaries from females maintained under simulated winter conditions for 28 days (see Methods). We also performed RNA-seq on ovaries from age-matched control females maintained at 25°C for 28 days. We prepared RNA from exclusively ovary stages 1-7 to ensure tissue homogeneity across all samples (Fig. 1B).

RNA-seq revealed distinct gene expression profiles of age-matched control ovaries (25°C), arrested ovaries (12°C), and persistently reproductive ovaries (12°C). As expected, the 200 most differentially

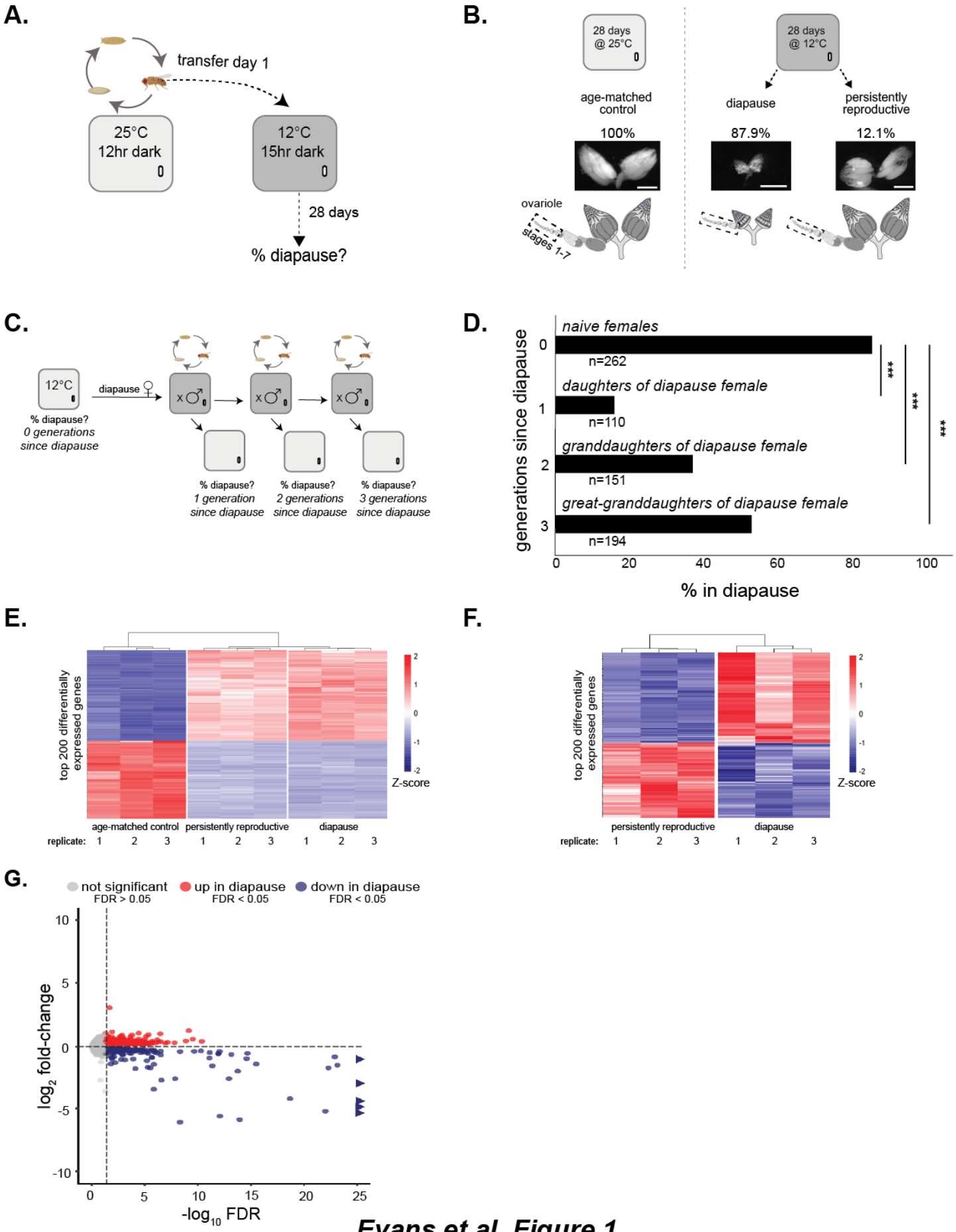

Evans et al. Figure 1

Figure 1. Establishing a system to study epigenetic regulation of developmental plasticity. (A) Diagram of diapause assay design. Flies are reared at 25°C under a 12-hour dark/light cycle in an incubator (light gray). Females are then transferred to an incubator set to 12°C under a 15-hour dark, 9-hour light cycle (dark gray, simulated winter conditions). Females are maintained in simulated winter conditions for 28 days before ovaries are assessed for diapause (% of females with arrested ovaries, i.e., "diapause plasticity"). (B) Degree of plasticity in age-matched control at 25°C (left) and diapause and persistently reproductive at 12°C (right). Ovaries from age-matched control females, diapause females, and persistently reproductive females and cartoons (below) representing the ovaries with a separated single ovariole, the basic unit of egg production in the *Drosophila* ovary. Dotted box indicates stages 1-7 used for all RNA and protein assays (note that the arrested ovary has only stages 1-7, created using Biorender.com). Scale bars = 0.5 mm (C) Diagram of transgenerational assay design. After maintenance under simulated winter conditions for 28 days (dark gray incubator, see above), females are assayed for diapause using a non-destructive method (see Methods). The females previously in diapause ("naïve females") are then crossed to males at 25°C. Virgin females from this cross ("daughters of diapause female") are placed either into a 12°C incubator to assess diapause plasticity or into a vial with males at 25°C to generate the granddaughters of diapause females. This process is repeated with these granddaughters and the great-granddaughters of diapause females. (D) Diapause plasticity of daughters, granddaughters, and great-granddaughters of females who underwent diapause. χ^2, *** $p<0.001$. (E) Heatmap of the top 200 differentially expressed genes (by FDR) between age-matched control, diapause, and persistently reproductive ovaries. Blue-red gradient depicts the Z-score of each gene. Red corresponds to upregulated genes and blue corresponds to downregulated genes. (F) Heatmap of top 200 differentially expressed genes (by FDR) between diapause and persistently reproductive ovaries. Blue-red gradient depicts the Z-score of each gene. Red corresponds to upregulated genes and blue corresponds to downregulated genes. (G) Volcano plot showing differential gene expression across arrested and persistently reproductive ovaries. Triangles represent genes with $-\log_{10}$ FDR > 25.

147 expressed genes (by false discovery rate, "FDR") are differentially expressed between age-matched
148 control ovaries at 25°C and ovaries at 12°C (Fig. 1E, Fig. S1A); however, within the 12°C treatment,
149 diapausing and persistently reproductive ovaries have distinct gene expression programs (Fig. 1F, Fig.
150 S1B). More genes are down-regulated than up-regulated in diapausing compared to persistently
151 reproductive ovaries, and more down-regulated genes have $\log_2$-fold change greater than two (Fig.
152 1G). Nevertheless, the significant upregulation of hundreds of genes in diapause suggests that *D.*
153 *melanogaster* diapause is not simply a generalized shut-down of gene expression but instead an
154 actively regulated state [see also (54)]. This differential gene expression between diapause and
155 persistently reproductive ovaries at 12°C, combined with the transgenerational effect of diapause,
156 suggests that epigenetic factors mediate reproductive arrest in the ovary.
157
158 *Epigenetic marks H3K4me3 and H3K36me1 regulate diapause plasticity*
159
160 Epigenetic regulation depends in part on chromatin modifications [reviewed in (55)]. The basic unit of
161 chromatin is the nucleosome, comprised of DNA wrapped around histone proteins that form an octamer
162 (56). Residues on the tails of histones can be post-translationally modified, primarily by the addition or
163 removal of acetyl and methyl groups (57). These histone marks can alter the transcriptional activity of
164 the underlying DNA [reviewed in (58)]. To identify histone marks associated with diapause plasticity, we
165 prepared lysate from arrested ovaries and persistently reproductive ovaries (stages 1-7) and screened
166 six, highly abundant histone H3 modifications (59). This screen revealed that H3K27me3, H3K27ac,
167 H3K9me3, and H3K9ac do not differ in abundance across diapausing and persistently reproductive
168 ovaries (Fig. 2A, Fig. S2). In contrast, H3K4me3 and H3K36me1 are depleted in diapause (Fig. 2A, Fig.
169 S2).
170
171 Variation in H3K4me3 and H3K36me1 abundance across diapausing and persistently reproductive
172 ovaries could reflect a causal role of histone marks in determining diapause plasticity. To test the
173 prediction that these marks in the ovary affect reproductive plasticity, we manipulated histone mark
174 abundance. Using the Gal4/UAS system (see Methods), we expressed in the ovary short hairpin RNAs
175 (shRNAs) that knockdown transcripts of enzymes that deposit or remove these histone marks (Fig.
176 2B,C). Given that diapause plasticity is well-known to vary across genotypes (41, 44, 60, 61), we strictly
177 controlled the genetic background of the experimental and control flies. To generate the experimental
178 lines, we introduced chromosomes carrying the focal shRNA construct, integrated into an attP landing
179 site, into the inbred line from Pennsylvania described above (Fig. 2B). To generate the control lines, we
180 introduced chromosomes that have the same attP landing site, but *lack* the shRNA construct, into the
181 same inbred line (Fig. 2B). We crossed these experimental and control lines to a driver line that directs
182 expression of the shRNA in the ovary.
183
184 We manipulated the abundance of three histone marks in the ovary and assayed diapause plasticity
185 (the percent of females with arrested ovaries) using these rigorously controlled genotypes. First, we
186 manipulated a "control" histone mark, H3K9me3, which does not vary between diapausing and
187 reproductive ovaries (Fig. 2A, Fig. S2). Specifically, we knocked down *JHDM2* (Fig. S3A), an enzyme
188 that demethylates H3K9. As expected, *JHDM2* knockdown elevated H3K9me3 (Fig. 2C) but had no
189 effect on diapause plasticity (Fig. 2D, odds ratio=0.846, $p>0.05$). Next, we manipulated H3K36me1 and
190 H3K4me3, two histone marks depleted in arrested ovaries (Fig. 2A). We predicted that experimental
191 depletion of these marks would increase diapause plasticity, while experimental enrichment would
192 decrease diapause plasticity. This is exactly what we observed. To deplete H3K36me1, we knocked
193 down *Set2*, which encodes an enzyme that methylates H3K36 (Fig. 2C, Fig. S3A). Indeed, H3K36me1
194 depletion increased diapause plasticity (Fig. 2D, odds ratio=10.35, $p<0.05$). Similarly, we depleted
195 H3K4me3 by knocking down *Set1*, which encodes an enzyme that methylates H3K4 (Fig. 2C, Fig. S3A)
196 and again observed increased diapause plasticity (Fig. 2D, odds ratio=29.19, $p<0.0001$). We then
197 experimentally *enriched* H3K4me3 by knocking down *lid*, which encodes an enzyme that removes
198 H3K4 methylation (Fig. 2C, Fig. S3A). As predicted, this opposing manipulation decreased diapause

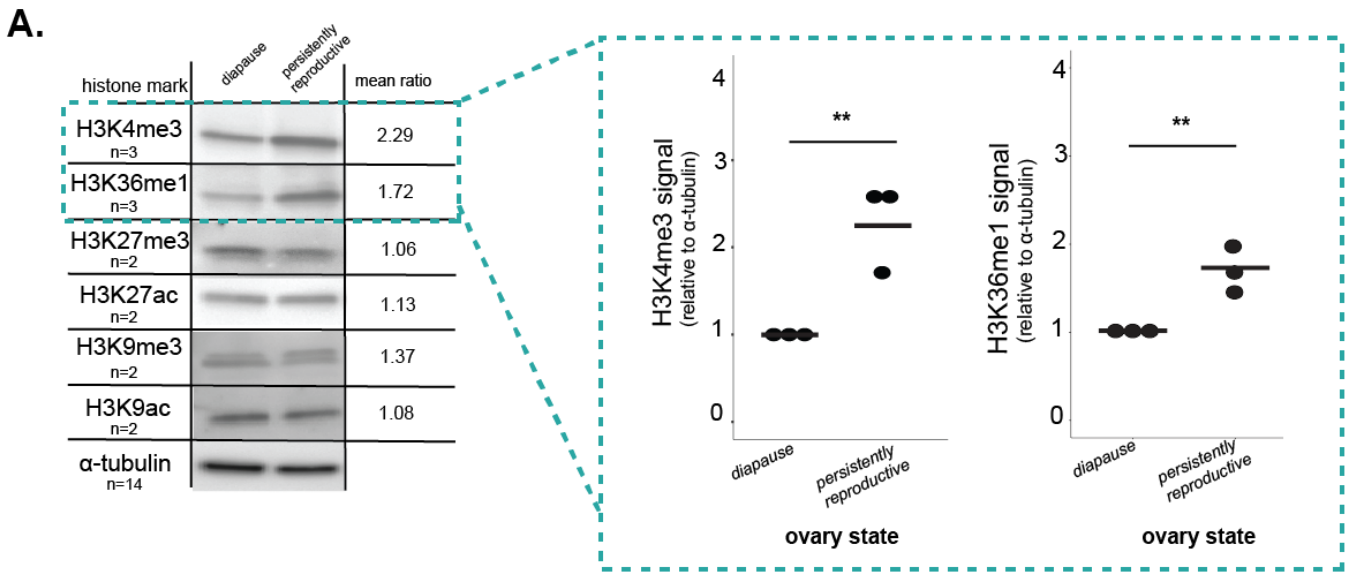

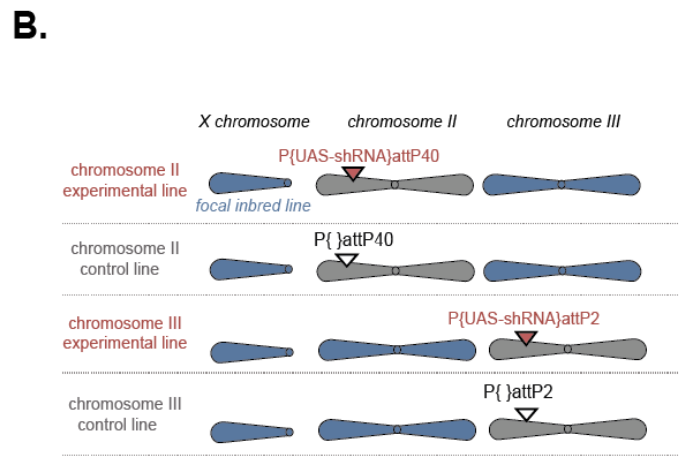

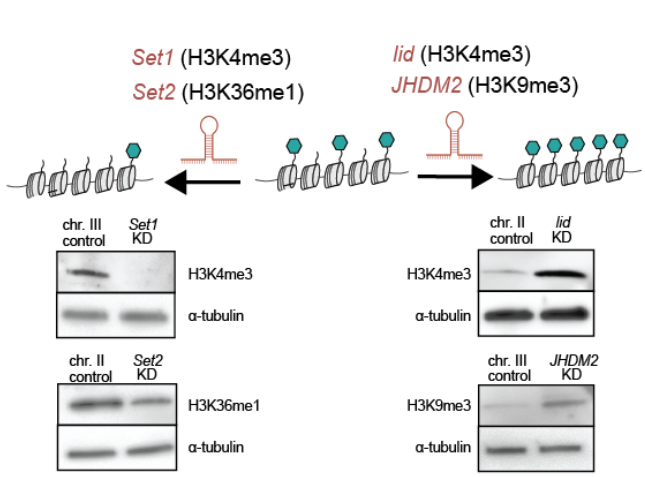

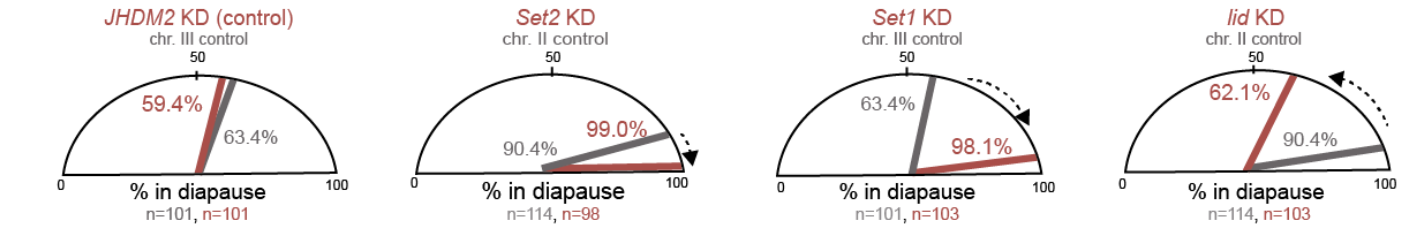

RNAi target	verified change in histone mark	change in diapause penetrance: expected	change in diapause penetrance: observed	control n	KD n	likelihood of change (odds ratio)
JHDM2	↑H3K9me3	no change	no change	101	101	0.846
Set2	↓H3K36me1	↑	↑	114	98	**10.35 ***
Set1	↓H3K4me3	↑	↑	101	103	**29.19 *****
lid	↑H3K4me3	↓	↓	114	103	**0.175 *****

Evans et al. Figure 2

199 **Figure 2. H3K4me3 and H3K36me1 regulate diapause plasticity.** (A) Representative western blots
200 showing histone mark abundance in diapausing and persistently reproductive ovaries. Quantification of
201 H3K4me3 and H3K36me1 signal relative to α-tubulin loading control for three biological replicates
202 (right). t-test, **$p < 0.01$. (B) Genotypes of experimental and control lines in histone mark manipulation
203 experiment. Blue chromosomes represent chromosomes from the focal inbred line. Experimental
204 genotypes encode a construct with a UAS promoter that drives a small hairpin RNA ("P{UAS-shRNA}").
205 These constructs are inserted into a chromosome-specific attP site (pink triangle). Control line attP
206 sites lack the inserted construct (white triangle). All lines are crossed to the same ovary-specific driver.
207 (C) Expected change of histone mark abundance after RNAi against histone mark writers and erasers
208 (above) and western blots validating histone mark depletion or enrichment (below). "chr." =
209 chromosome. (D) Diapause plasticity of experimental (pink) and control (gray) genotypes. Expected
210 direction of change shown with a black dotted arrow. FET, * $p < 0.05$, *** $p < 0.001$. "chr." =
211 chromosome. Note that we ruled out the possibility that diapause-independent effects of knockdown of
212 *Set1* and *Set2* on ovary development confounded these results (see Methods and Fig. S3B)

213

214 plasticity (Fig. 2D, odds ratio=0.175, $p<0.0001$). These data suggest that H3K36me1 and H3K4me3
215 depletion, but not H3K9me3 elevation, promotes diapause plasticity
216
217 *Diapause-associated chromatin state and gene expression are genotype-specific*
218
219 We found that the chromosome II and chromosome III control genotypes have strikingly different
220 diapause plasticity despite no gene knockdown (63.4% in chromosome II control, 90.4% in
221 chromosome III control, Fig. 2D). This observation suggests that diapause plasticity is exquisitely
222 sensitive to genotypic variation, an inference consistent with previous reports of natural genetic
223 variation in diapause plasticity (41, 60, 62). Moreover, diapause plasticity is known to decrease linearly
224 along the east coast of the United States (44) such that isofemale lines collected from temperate
225 Pennsylvania have higher incidence of diapause than lines collected from subtropical Florida (when
226 exposed to simulated winter conditions). This genetic variation for diapause plasticity, combined with
227 the discovery that H3K4me3 and H3K36me1 are depleted in arrested ovaries from a highly plastic line
228 derived from temperate Pennsylvania, raised the possibility that the epigenetic determinants of
229 diapause plasticity may also vary across genotypes. To begin to test this possibility, we derived an
230 additional inbred line from an isofemale line collected from subtropical Florida, a region that lacks
231 severe winters. As expected, this inbred line has low diapause plasticity (14.9% diapause, Fig. 3A).
232 Henceforth, we refer to the temperate inbred line described above as "High Plasticity" or "HP" (87.9%
233 diapause), and the subtropical inbred line as "Low Plasticity" or "LP".
234
235 Given that the LP line is largely insensitive to the simulated winter conditions, we first determined
236 whether diapause in the LP line is a *bona fide* alternative developmental state or instead a generalized
237 stress response to simulated winter conditions [see (63)]. Previous studies have demonstrated that
238 diapause preserves fertility and germline stem cell number compared to age-matched controls, while
239 stress does not (46). Diapausing ovaries also accumulate the double-strand break marker, γ-H2av, due
240 to the persistence of egg chambers in extended arrest (46). We found that despite low responsiveness
241 to simulated winter conditions, the LP line, like the HP line, preserves germline stem cell number (Fig.
242 3B) in diapause compared to age-matched controls. Furthermore, LP and HP diapausing ovaries are
243 similarly enriched for γ-H2av compared to age-matched controls (Fig. 3C). Diapause also preserves
244 fertility in the LP line compared to age-matched controls (Fig. S4). These data suggest that the LP line
245 enters a true diapause state in response to simulated winter conditions.
246
247 We hypothesized that genetic variation for diapause plasticity across the HP and LP line shape the
248 epigenetic determinants of diapause plasticity. To test this hypothesis, we screened ovaries of the LP
249 line for the same six histone marks screened in the HP line. Similar to the HP line, H3K9ac, H3K9me3,
250 H3K27ac and H3K27me3 abundance did not differ between diapausing and persistently reproductive
251 ovaries of the LP line (Fig. S2). However, unlike the H3K4me3 and H3K36me1 depletion that we
252 observed in diapausing ovaries of the HP line, these two marks were invariant across the two
253 developmental fates in the LP line (Fig. 4A). These data are consistent with the hypothesis that the
254 chromatin state of diapausing ovaries is distinct in the HP and LP lines, and suggest that a distinct
255 chromatin mark(s), or chromatin-independent epigenetic factors, determine diapause plasticity in the LP
256 line.
257
258 Depletion of H3K4me3 and H3K36me1 in the HP line, but not in the LP line, suggests that these two
259 genotypes harbor different H3K4me3 and H3K36me1 genome-wide profiles under diapause conditions.
260 To test this prediction, we attempted to use CUT&RUN, a genome-wide chromatin profiling approach
261 that requires minimal sample material (64). Unfortunately, attempts to profile the minimal tissue from
262 stages 1-7 of the diapausing and persistently reproductive ovaries were unsuccessful. We turned
263 instead to gene expression, reasoning that genotype-dependent histone mark abundance in diapause
264 may promote genotype-dependent gene expression. Alternatively, gene expression might be entirely
265 genotype-independent, showing sensitivity only to reproductive state. In this case, the same genes

A

reproductive state @ 12˚C	high plasticity (HP) inbred line * n=282	low plasticity (LP) inbred line n=242
diapause	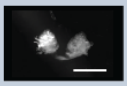	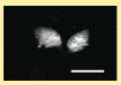
persistently reproductive	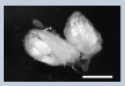	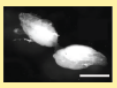
% in diapause	87.9%	14.9%

** see also Figure 1B*

B

representative images of germline stem cell quantification

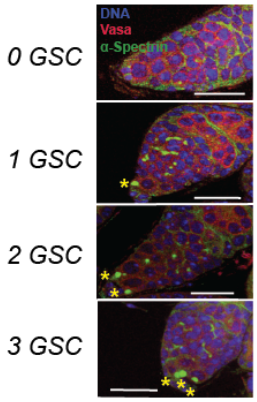

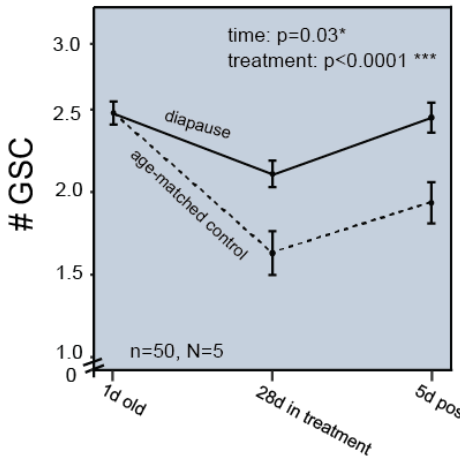

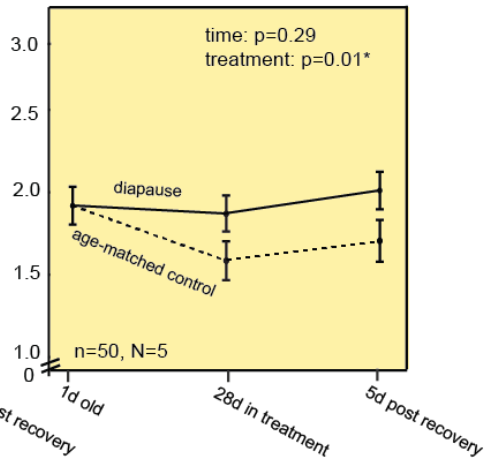

C

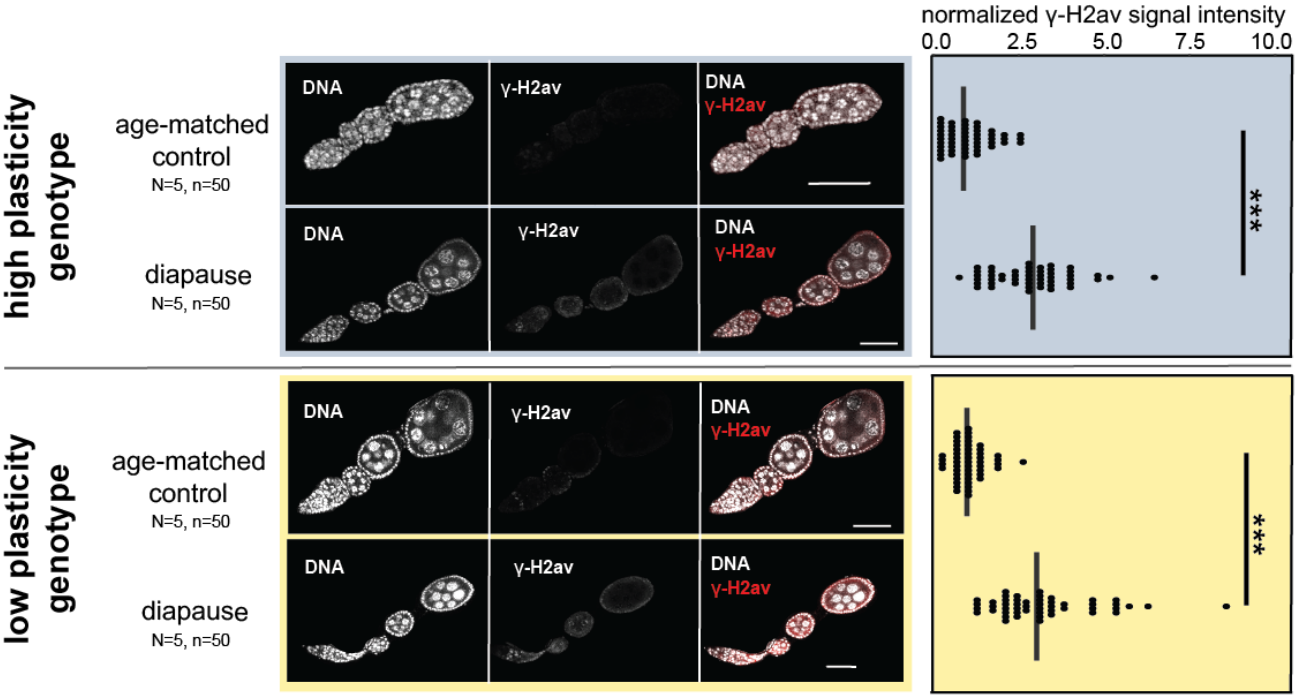

Evans et al. Figure 3

266 **Figure 3. Assessing the diagnostic features of diapause in a low plasticity genotype.** (A)
267 Representative images of diapausing and persistently reproductive ovaries of high plasticity (HP, blue)
268 and low plasticity (LP, yellow) inbred lines as well as the degree of plasticity (note: HP % diapause was
269 previously reported in Figure 1B). Scale bar = 0.5 mm. (B) Representative images of germaria with 0, 1,
270 2, and 3 germline stem cells ("GSC," designated by *, scale bar = 10μm) stained with DAPI (blue), anti-
271 Vasa (red) and anti-α-Spectrin (green). Average number of germline stem cells at one day old, after 28
272 days of treatment (25°C or 12°C), and after five days post-treatment at 25°C for diapausing and age-
273 matched control ovaries of HP and LP females (scale bar = 25μm, d="day", 2-way ANOVA with fixed
274 effects = timepoint, treatment, error bars = SEM). (C) γ-H2av signal in age-matched control and
275 diapausing ovaries of HP and LP females and quantification. Mann-Whitney U test, *** $p<0.001$, scale
276 bar = 50μm.

277

278 would be differentially expressed across diapausing and persistently reproductive ovaries in both LP
279 and HP lines.
280
281 To investigate the diapause-associated gene expression program between the LP and HP lines, we
282 conducted RNA-seq on the LP line (Fig. S5). To isolate those genes that are up- and down-regulated
283 specifically in diapause, we normalized the list of genes that were differentially expressed between
284 diapausing and persistently reproductive ovaries (both at 12°C) to gene expression of age-matched
285 control ovaries (25°C). Specifically, we included in downstream analyses only those genes that were
286 differentially expressed between diapausing and persistently reproductive ovaries *and* between
287 diapausing and age-matched control ovaries in a given genotype. We compared this reduced list of
288 diapause-specific genes across the two genotypes (433 in HP, 606 in LP) and determined which genes
289 were differentially expressed in both HP and LP ("genotype-independent"), differentially expressed only
290 in the HP line ("HP-specific"), or differentially expressed only in the LP line ("LP-specific"). While many
291 genes that are up- or down- regulated in diapause are shared across the HP and LP lines (201 genes,
292 Fig. 4B), most differentially expressed genes are genotype-dependent (611 genes, Fig. 4B). These
293 results further suggest that HP and LP diapause plasticity may be regulated by distinct mechanisms.
294
295 The observation of pervasive genotype-dependent gene expression associated with a common
296 phenotype suggests functional convergence. We hypothesized that distinct genes in the same
297 pathways are associated with diapause in each genotype. Consistent with this prediction, we found
298 evidence that genotype-dependent gene expression in HP and LP diapause converges on common
299 biological processes. For example, two metabolic pathways are enriched in both HP-specific and LP-
300 specific genes up-regulated in diapause (Table 1, highlighted in green). Moreover, twelve pathways are
301 enriched for *both* genotype-independent genes and genotype-*dependent* genes upregulated in
302 diapause (Table 1, highlighted in gray). This finding suggests that some pathways are utilized by both
303 genotypes via the expression of overlapping genes *and* non-overlapping genes. There were no
304 significant pathways overrepresented for genes downregulated in HP-dependent and only a single
305 pathway overrepresented for genotype-independent downregulated genes; consequently, common
306 pathways could not be detected for down-regulated genes. These results suggest that diapause in both
307 genotypes may depend on the activation of the same pathways but through a distinct set of genes,
308 regulated by distinct epigenetic mechanisms.
309

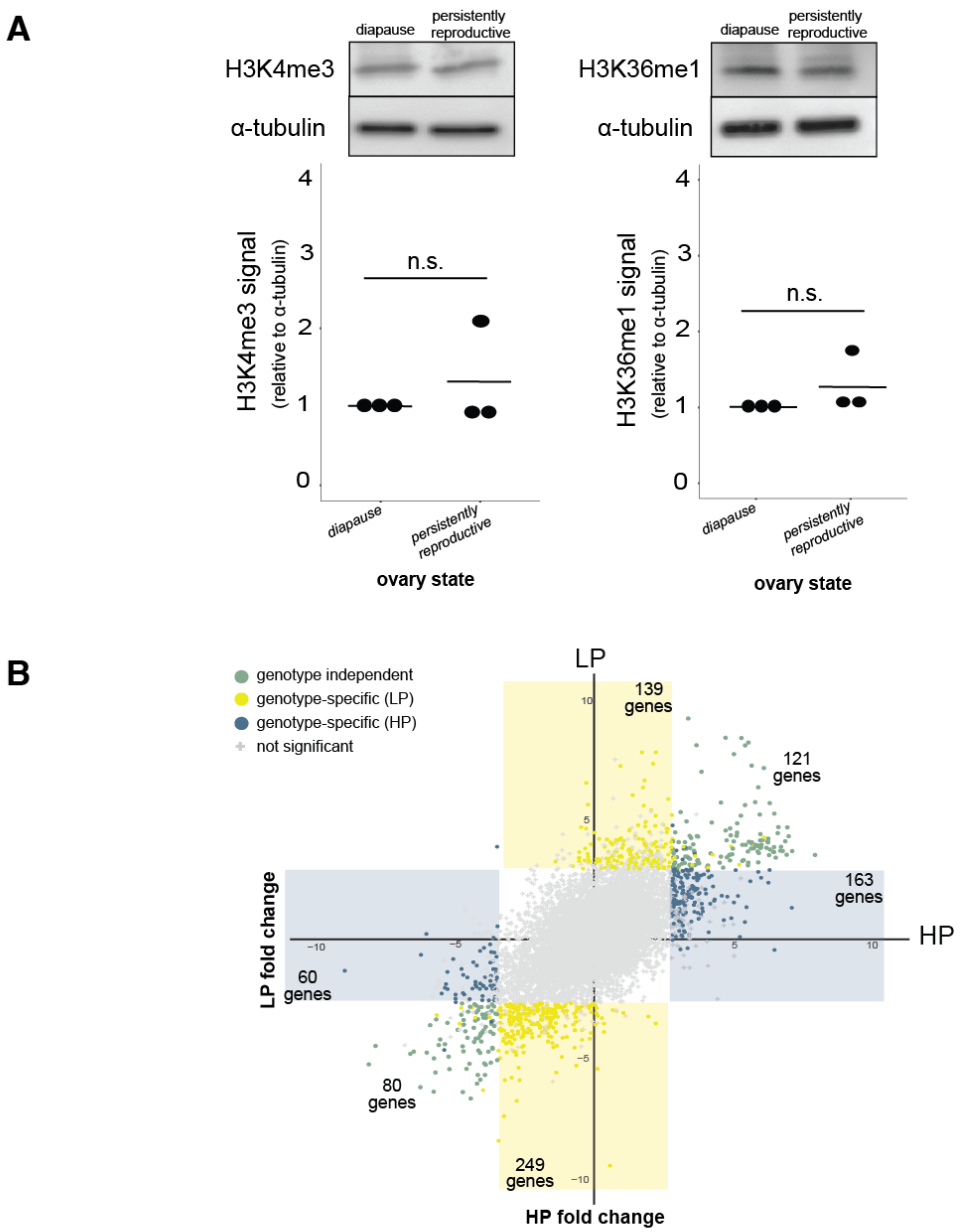

Evans et al. Figure 4

Figure 4. Diapause-associated chromatin state and diapause-associated gene expression are genotype-specific. (A) Representative western blots showing the abundance of H3K4me3 and H3K36me1 in diapausing and persistently reproductive ovaries from the LP inbred genotype females (above). Quantifications of H3K4me3 and H3K36me1 signal relative to α-tubulin loading control for three replicates (below). t-test, n.s. = p>0.05, (compare to Figure 2A). (B) Differential gene expression across diapausing and persistently reproductive ovaries in HP and LP genotypes. Gray points represent genes that are not significantly differentially expressed in either genotype. Green points represent genes that are differentially expressed in both genotypes (FDR < 0.05). Blue points represent genes that are differentially expressed in the HP genotype only (FDR < 0.05). Yellow points represent genes that are differentially expressed in the LP genotype only (FDR < 0.05).

320 **Table 1. Pathway enrichment for genes up-regulated in diapause.** Gray pathways are significant in
321 all categories (genotype-independent, HP-specific and LP-specific genes). Green pathways are
322 significant in both HP-specific and LP-specific genes. Blue pathways are significant in both genotype-
323 independent and HP-specific genes. No pathways are significant in both genotype-independent and
324 LP-specific genes.

Pathway	genotype-independent (FDR)	HP-specific (FDR)	LP-specific (FDR)
GTP hydrolysis and joining of the 60S ribosomal subunit (R-DME-72706)	4.08E-102	4.21E-03	4.20E-02
SRP-dependent cotranslational protein targeting to membrane (R-DME-1799339)	3.82E-101	5.49E-03	4.99E-02
Nonsense Mediated Decay (NMD) independent of the Exon Junction Complex (EJC) (R-DME-975956)	1.38E-100	6.25E-03	1.68E-02
Formation of a pool of free 40S subunits (R-DME-72689)	1.58E-99	3.93E-06	3.12E-03
L13a-mediated translational silencing of Ceruloplasmin expression (R-DME-156827)	1.87E-99	4.95E-06	1.43E-03
Eukaryotic Translation Initiation (R-DME-72613)	4.93E-98	6.47E-06	1.46E-03
Cap-dependent Translation Initiation (R-DME-72737)	5.54E-98	7.76E-06	1.82E-03
Nonsense Mediated Decay (NMD) enhanced by the Exon Junction Complex (EJC) (R-DME-975957)	5.61E-98	1.17E-02	2.24E-02
Nonsense-Mediated Decay (NMD) (R-DME-927802)	6.55E-98	1.23E-02	2.41E-02
Translation (R-DME-72766)	1.99E-84	1.98E-05	1.43E-03
Metabolism of RNA (R-DME-8953854)	1.26E-70	1.85E-03	1.84E-03
Metabolism of proteins (R-DME-392499)	1.62E-47	5.59E-05	1.76E-02
The citric acid (TCA) cycle and respiratory electron transport (R-DME-1428517)	n.s.	8.59E-04	1.49E-02
Respiratory electron transport, ATP synthesis by chemiosmotic coupling, and heat production by uncoupling proteins. (R-DME-163200)	n.s.	2.92E-03	2.88E-02
Ribosomal scanning and start codon recognition (R-DME-72702)	1.08E-38	5.60E-06	n.s.
Translation initiation complex formation (R-DME-72649)	1.52E-38	5.56E-06	n.s.
Activation of the mRNA upon binding of the cap-binding complex and eIFs, and subsequent binding to 43S (R-DME-72662)	2.13E-38	5.60E-06	n.s.
Formation of the ternary complex, and subsequently, the 43S complex (R-DME-72695)	3.94E-38	5.79E-06	n.s.
rRNA processing in the nucleus and cytosol (R-DME-8868773)	2.66E-20	3.76E-02	n.s.
rRNA processing (R-DME-72312)	2.80E-20	3.90E-02	n.s.
Major pathway of rRNA processing in the nucleolus and cytosol (R-DME-6791226)	2.97E-20	4.05E-02	n.s.
Metabolism (R-DME-1430728)	n.s.	1.16E-05	n.s.
Signaling by Nuclear Receptors (R-DME-9006931)	n.s.	3.92E-02	n.s.
Metabolism of amino acids and derivatives (R-DME-71291)	n.s.	4.42E-02	n.s.
mRNA Splicing (R-DME-72172)	n.s.	n.s.	2.91E-02
mRNA Splicing - Major Pathway (R-DME-72163)	n.s.	n.s.	3.04E-02

DISCUSSION

Here we describe a new, tractable system for studying the role of chromatin in regulating developmental plasticity. Importantly, this model system controls for the confounding effects of genetic variation, environment, and tissue heterogeneity on chromatin packaging, allowing us to isolate functional links between chromatin modifications and developmental fate. We discovered that environment-dependent reproductive arrest in *D. melanogaster* is mediated by at least two histone marks, H3K4me3 and H3K36me1. We also found that this epigenetic mechanism may be genotype-specific – these two marks were depleted in diapausing ovaries of a temperate, high plasticity genotype but were similarly abundant across diapausing and reproductive ovaries in a subtropical, low plasticity genotype. These data raise the possibility of a distinct epigenetic basis of diapause plasticity across distinct genotypes.

Previous studies in non-model or emerging model systems have demonstrated compelling causal links between chromatin and diapause. Two major chromatin silencing pathways emerged from these studies: DNA methylation in *Nasonia* wasps (34) and H3K27me3 in the Cotton bollworm moth (33) and the Turqoise killifish (31). *D. melanogaster* has minimal DNA methylation (65); consequently, we focused on histone marks like H3K27me3. Surprisingly, the screen of histone marks revealed no difference in abundance of H3K27me3 between arrested and persistently reproductive ovaries [as was found in bollworm pupa (33)], and we did not detect differential expression of enzymes that write, read, or erase H3K27me3 [as was found in killifish embryos (31)]. These observations implicated a distinct chromatin mechanism regulating *D. melanogaster* reproductive diapause. Our focus on the ovary may account for this difference. These prior studies probed the paused developmental transitions during juvenile phases, either embryonic or larval, rather than the adult reproductive tissue. H3K27me3 may mediate *D. melanogaster* diapause in non-reproductive tissues like the brain, which also enters an alternative state during diapause (54). The notion that distinct histone marks regulate distinct tissues undergoing developmentally plastic responses is not unprecedented. Ozawa *et al.* (2016) identified distinct chromatin mechanisms of starvation-induced phenotypic plasticity across developing beetle wings and developing mandibles (29). Of course, we cannot yet rule out the possibility that H3K27me3, along with H3K4me3 and H3K36me1, regulates ovary arrest but gross H3K27me3 abundance does not vary between reproductive states.

The discovery that H3K4me3 depletion promotes reproductive diapause is reminiscent of earlier studies of somatic aging. From yeast to mammals, aging is associated with a general increase in active chromatin marks like H3K4me3 and an overall increase in transcription [reviewed in (66)]. In *Drosophila,* H3K4me3 depletion extends lifespan (67). Like these studies of somatic aging, we found not only that depletion of the active mark H3K4me3 promotes reproductive diapause but also that diapause is associated with a genome-wide decrease in gene expression. These results suggest that the chromatin state of the diapausing ovary mirrors that of young somatic tissues. Given that the chromatin determinants of age-dependent reproductive decline (68) are not nearly as well explored as the determinants of somatic aging [reviewed in (66, 69)], this study offers a new foothold for understanding how youthful chromatin state contributes to the preservation of reproductive potential.

Chromatin mediates not only development and aging within a generation but also mediates epigenetic information transfer between generations [reviewed in (70, 71)]. Our discovery of distinct epigenetic states between arrested and persistently reproductive ovaries raised the possibility that information about the maternal environment is transferred to the next generation. Consistent with diapause-induced transmission of epigenetic information, we found that diapause entry reduces subsequent diapause plasticity of genetically identical daughters, granddaughters, and great-granddaughters. Such transgenerational memory requires a DNA sequence-independent “message” to be passed from parent to offspring through the germline. The identity of this message remains mysterious; however, we speculate that either alternative chromatin packaging or specific transcripts, possibly small RNA(s) (72,

73), of diapausing ovaries transmits this heritable epigenetic information. The discovery of transgenerational information transfer from mother to daughter – in a model system – puts forward *D. melanogaster* diapause as a powerful new resource for studying epigenetic inheritance.

To isolate the role of sequence-independent, epigenetic determinants of diapause plasticity, we reduced genetic variation by inbreeding. However, *D. melanogaster* diapause, like other developmentally plastic phenotypes, varies across genotypes (41, 44, 60, 62, 74, 75). For example, aphid wing presence/absence is a developmentally plastic phenotype that depends on both maternal crowding environment and genotype. Maternal crowding induces wing development in progeny to different degrees, with some genotypes producing 0% and others 100% winged aphids (76). Similarly, epigenomic profiles also vary across genotypes. In human B cells, *Arabidopsis* leaves, and various maize tissues, the level and distribution of DNA methylation varies across individuals derived from natural populations (77-79). Similarly, genome-wide H3K4me3 distribution in the heart and liver varies across rat strains, and H3K27me3 distribution varies across seedlings from naturally derived *Arabidopsis* genotypes (80, 81). However, links between epigenetic variation and genetic variation in developmental plasticity are virtually unexplored (82). Here we found that epigenetic marks associated with diapause differ across naturally varying genotypes, raising the enticing possibility that the chromatin determinants of diapause in these genotypes are distinct. Unfortunately, the sensitivity of diapause plasticity to genetic background precluded us from testing directly the hypothesis that the low plasticity, subtropical derived line is insensitive to H3K4me3 and H3K36me1 manipulation. Future research implementing genome-wide chromatin profiling paired with transcriptomics, across many distinct genotypes, will offer new traction for testing this possibility.

Developmental plasticity allows individual organisms to better match a changing local environment. Importantly, many taxa occupy a broad range of local environments. Genetic variation for developmental plasticity across a species range allows distinct populations to respond differently to distinct local environments. *Drosophila melanogaster* diapause is exemplary. Diapause plasticity is high in populations from temperate regions with warm summers and cold winters, but low in populations from subtropical regions with warm summers and mild winters (43). Moreover, diapause plasticity is high in populations collected in the early spring, but low in populations collected in late summer (83). This adaptive temporal and spatial variation in diapause plasticity, paired with the discovery of epigenetic modulation of diapause plasticity reported here, raises the possibility that distinct epigenetic factors are selected to confer distinct degrees of diapause plasticity. Intriguingly, genes encoding many epigenetic factors exhibit latitudinal clines, including enzymes that methylate and demethylate H3K4 and H3K36 (84-86). This system is now well-positioned to offer the first glimpses of how adaptive evolution shapes epigenetic mechanisms underlying developmental plasticity. Such genetic variation of epigenetic regulation likely shapes how natural populations respond to the extreme seasonal environments arising from ongoing climate change (87).

MATERIALS AND METHODS

Drosophila **stocks and culturing**

We constructed the High Plasticity ("HP") inbred line from an isofemale line collected from Media, Pennsylvania in July, 2018. To inbreed the line, we mated one brother and one sister each generation for 10 generations. We similarly constructed the Low Plasticity ("LP") line from an isofemale line collected in Miami, Florida in July 2018. We maintained stocks at 25°C in 12-hour light/dark cycles on standard molasses food.

Diapause assay

To assay diapause, we subjected 0-6 hour-old virgin females to 12°C and a short-day light cycle (9 hours of light, 15 hours of darkness) for 28 days. To assay whether a female was in diapause, we dissected out the ovaries and determined the latest developmental stage of the ovary according to (88).

429 Specifically, as defined in Saunders *et al*. (1989), we designated females as undergoing diapause if
430 they lacked vitellogenic egg chambers (stage 8 or later, Fig. 1B). We designated females as
431 "persistently reproductive" if both ovaries had one or more egg chambers at stage 8 or later. We
432 excluded from experiments those rare females (<1%) whose ovaries fell between these categories.
433
434 **Transgenerational assay**
435 To assess transgenerational effects of diapause, we induced diapause as described above but
436 determined the reproductive state of females without dissection using a modification of the "Bellymount"
437 protocol described in (89). We positioned females between two cover slips with a drop of 50% glycerol
438 and determined the reproductive state by visualizing through the abdomen the presence or absence of
439 egg chambers at stage 8 or later. We then crossed females in diapause ("naïve females", Fig. 1C,D) to
440 males from the same inbred line at 25°C. We placed virgin female offspring from this cross either into a
441 12°C incubator ("daughters of diapause females," Fig. 1C,D) to assess diapause rate or into a vial with
442 males at 25°C to generate granddaughters of the generation 0 diapause females. We repeated this
443 process with these granddaughters as well as the great-granddaughters of the generation 0 diapause
444 ("naïve") females. We compared diapause plasticity of generation 0 to that of daughters,
445 granddaughters, and great-granddaughters using χ^2 test.
446
447 **RNA-sequencing and analysis**
448 To define the gene expression associated with diapause while controlling for genotype, temperature,
449 and age, we induced diapause as described above. We kept age-matched control flies as virgins in an
450 incubator set to 25°C and a long day light cycle (12 hours of light, 12 hours of dark) for 28 days. We
451 flipped these control females onto fresh food every 7 days due to accelerated mold growth on the food
452 at 25°C. We isolated equivalent egg chamber stages from ovaries across reproductive states. For
453 persistently reproductive ovaries and age-matched control ovaries, we dissected off accessory
454 structures and then isolated by microdissection ovary stages 1-7 only (Fig. 1B). For arrested ovaries,
455 we removed the accessory structures only. We prepared total RNA (Mirvana miRNA isolation kit,
456 Thermo Fisher, Waltham, MA) from three replicates of 50 pooled ovaries for each condition in each
457 genotype. In total, we prepared 18 samples (HP diapause, HP persistently reproductive, HP age-
458 matched control, LP diapause, LP persistently reproductive, and LP age-matched control) and 18
459 libraries using NEBNext Ultra II (directional) with Poly-A selection, and sequenced libraries using
460 Illumina 2x150 for a total of 30M reads per sample (Admera Health Biopharma Services, South
461 Plainfield, NJ). All sequencing reads are available on the Sequencing Read Archive (NCBI), accession
462 number PRJNA884433.
463
464 We trimmed raw reads using Trimmomatic (v.0.39) (90) and mapped reads to the *D. melanogaster*
465 reference transcriptome using STAR aligner (v.2.7.10) (91). We estimated expression levels using
466 FeatureCounts (v.2.0.3) (92) and analyzed differential expression using DESeq2 (v.1.36.0) in R (93).
467 We discarded genes with fewer than 50 reads total across all samples in these analyses. We defined
468 genes as significantly differentially expressed if the false discovery rate (FDR) was less than 0.05.
469 Upon analyzing differential expression, we found that six and seven genes in the HP and LP lines,
470 respectively, were significantly differentially expressed between diapausing and persistently
471 reproductive ovaries (FDR < 0.05) but had a high standard error (lfcSE >1). In both genotypes, only a
472 single replicate of the (pooled) persistently reproductive ovaries had an elevated number of reads
473 mapping to these genes. We discovered that these genes belong to the multi-copy chorion gene
474 cluster, which undergoes selective, 15-80-fold, gene amplification (endo-replication) in the ovarian
475 follicle cells from ovary stages 8-14 (94). This observation is consistent with a small amount of
476 contamination of a later stage egg chamber. Indeed, the chorion genes accounted for the unusual
477 deviation of the single replicate from the other two replicates in both genotypes. Furthermore, excluding
478 these genes had no effect on the conclusions drawn from the data.
479

To compare diapause-specific gene expression between the HP and LP lines, we used the age-matched control ovaries to normalize genes that were differentially expressed between diapausing and persistently reproductive ovaries. We included in downstream analyses only those genes that were differentially expressed between diapausing and persistently reproductive ovaries *and* between diapausing and age-matched control ovaries in a given genotype. In other words, we excluded genes that are specifically up- or down-regulated in persistently reproductive ovaries compared to both diapause and age-matched controls. After generating this reduced list of significantly differentially expressed genes for both HP and LP genotypes, we compared across the two gene lists and determined which genes were differentially expressed in both HP and LP ("genotype-independent"), differentially expressed only in the HP line ("HP-specific"), or differentially expressed only in the LP line ("LP-specific", see Fig. 4B).

We performed pathway enrichment analysis of differentially expressed genes using the Reactome Pathway Database (v.81) (95) We considered pathways significantly enriched if there were five or more genes in a given category and the FDR was less than 0.05.

Western blotting and analysis

To assay histone mark abundance in the ovary, we isolated by microdissection ovary stages 1-7 (see above) in 1X PBS and ground the material in RIPA buffer (Cell Signaling Technology, Danvers, MA), Protease Inhibitor Cocktail (Roche, Basel, Switzerland), and PMSF (Cell Signaling Technology, Danvers, MA). To promote solubility, we incubated the lysate in Benzonase (Sigma Aldrich, St. Louis, MO) for 30 min at 4°C. We probed the blots with anti-H3K4me3 (Active Motif, Carlsbad, CA), anti-H3K36me1 (Abcam, Cambridge, UK), anti-H3K27me3 (Active Motif, Carlsbad, CA), anti-H3K27ac (Abcam, Cambridge, UK), anti-H3K9me3 (Abcam, Cambridge, UK), and anti-H3K9ac (Abcam, Cambridge, UK) at 1:1000 dilution. We probed with anti-α-tubulin (Developmental Studies Hybridoma Bank, Iowa City, IA) as a loading control (also 1:1000 dilution). We used anti-mouse and anti-rabbit HRP secondaries (Kindle Biosciences, Greenwich, CT) both at 1:1000. We exposed the blots with Kwikquant western blot detection kit and imaged with a Kwikquant imager (Kindle 277 Biosciences, Greenwich, CT). We quantified relative fluorescence of marks according to Stael *et al*. (2022*)* and normalized all measurements to diapause (96). We ran a third biological replicate only if we detected consistent differences in abundance across two replicates. For marks H3K4me3 and H3K36me1, we ran three biological replicates and compared abundance across diapausing and reproductive ovaries using Mann-Whitney U test.

Tissue-specific knockdown of histone writers and erasers and analysis of diapause plasticity

To knockdown expression of histone mark writers and erasers, we took advantage of preconstructed D. melanogaster lines from the Transgenic RNAi Project (97). These lines encode "Upstream Activating Sequence" (UASp)-driven short hairpins (shRNA) that target transcripts encoding D. melanogaster JHDM2 (Bloomington Drosophila Stock Center "BDSC" #32975), Set2 (BDSC #55221), Set1 (BDSC #33704), and lid (BDSC #36652). These cassettes are inserted into attP landing sites. Given the well-known effects of genetic background on diapause plasticity (41, 44, 60, 62), we carefully introgressed the chromosome encoding each UASp-shRNA construct (Set2 and lid on chromosome II, JHDM2 and Set1 on chromosome III) into the HP inbred line (see Fig. S6 for crossing scheme). Furthermore, we ensured no recombination using a combination of balancer chromosomes and transmission only through males (which do not recombine) to tightly control the genetic background of the control and experimental flies (Fig. S6). Moreover, we only compared experimental genotypes encoding the UASp-shRNA construct in a given attP site to control genotypes encoding the same chromosome encoding the same attP site but lacking the UASp-shRNA construct (BDSC #36304 for chromosome II, BDSC #36303 for chromosome III). To verify the presence of these constructs after the multi-generation crossing scheme, we used PCR to amplify the AmpR gene introduced along with the UAS-shRNA construct (Table S1). We crossed these stable stocks to the MTD-Gal4 driver (BDSC #31777), which expresses the GAL4 transcription factor throughout the ovary (98).

To validate the knockdown of transcription by RNAi, we performed RT-qPCR on RNA prepared from ovaries stages 1-7 in control and experimental shRNA genotypes at 48 hours after eclosion at 25°C (Table S1). To validate the depletion or enrichment of histone mark abundance by RNAi against the target chromatin writers and erasers, we conducted western blotting (as above) on protein lysate prepared from stages 1-7 ovaries from control and experimental shRNA genotypes 48 hours after eclosion at 25°C. We note that interpreting assays of histone marks at 12°C in genotypes with active RNAi is technically unfeasible. Temperature has a profound effect on histone mark distribution across the genome (27, 99, 100). Consequently, assaying histone mark abundance in these genotypes at 12°C would confound the effects of transcript knockdown and temperature. We also note RNAi efficiency decreases with decreasing temperature (101, 102), disabling us from distinguishing between the effects of RNAi on diapause entry and maintenance.

To determine whether experimental manipulation of histone mark abundance altered diapause plasticity, we assayed diapause in control and experimental RNAi lines by dissecting ovaries after 28 days in diapause-inducing conditions, as described above. We analyzed diapause plasticity using an odds ratio, which represents the change in likelihood of diapause given the presence of transcript knockdown. We used a Fisher's Exact Test (implemented in R) to compare diapause plasticity between control and RNAi lines.

D. melanogaster ovary development depends in part on chromatin-mediated gene regulation. We sought to rule out the possibility that the observed increase in incidence of arrest ("diapause plasticity") upon transcript knockdown was simply due to a block in ovary development, independent of diapause. This was of particular concern given that experimental depletion of H3K36me1 and H3K4me3 increased diapause to nearly 100%. We reasoned that increasing the dynamic range of diapause plasticity in both experimental and control lines could allow us to determine if ovary development was blocked upon transcript knockdown at 12°C. To decrease the baseline diapause plasticity in both experimental and control lines, we took advantage of the transgenerational decrease in diapause plasticity (Fig. 1D). We exposed females from the UAS-shRNA and control lines to diapause conditions and assayed ovary development using the modified Bellymount method described above. We then crossed females in diapause to the MTD-Gal4 driver (BDSC #31777), and exposed daughters from this cross to simulated winter conditions and assayed for diapause plasticity. We found that fewer than 20% of these daughters have arrested ovaries, suggesting that Set1 or Set2 knockdown alone does not block ovary development at 12°C (Fig. S3B).

Immunofluorescence and image analysis

To evaluate whether the LP line entered canonical diapause similarly to the temperate HP line, we conducted immunofluorescence on ovaries following (103). To assay germline stem cell number, we stained ovaries with anti-α-spectrin (1:300, Developmental Studies Hybridoma Bank, Iowa City, IA) and anti-Vasa (1:50, Developmental Studies Hybridoma Bank, Iowa City, IA). Following criteria described in (104), we defined germline stem cells as the anterior-most Vasa-positive cells in the stem cell niche that display an anterior α-spectrin signal (spectrosome). Scanning through each z-stack, we counted the number of germline stem cells from 10 germaria in 5 ovary pairs, for a total of 50 germaria. We used a 2-way ANOVA to evaluate the statistical significance of the effects of treatment (diapause and age-matched control) and time (28 days in treatment vs. 5 days recovered from treatment). To assay double-strand break abundance, we stained ovaries with anti-γ-H2Av (1:1000, Developmental Studies Hybridoma Bank, Iowa City, IA). To quantify the average fluorescence of γ-H2Av in ovaries, we outlined representative stage 4 egg chambers with the Freehand tool in FIJI (v.1.0) (105). Also in FIJI, we calculated the fluorescent signal intensity using the polygon tool to define the borders of the tissue. We used the "measure tool" to calculate the mean pixels within these boundaries. We normalized all fluorescence intensity values of the HP line to the mean intensity value of the age-matched control in HP, and all fluorescence intensity values of the LP line to the mean intensity value of the age-matched

control in LP. We calculated fluorescence from 10 replicates of stage four egg chambers in five ovary pairs, for a total of 50 egg chambers. We compared the mean fluorescence of γ-H2av in diapause and age-matched control ovaries using a Mann-Whitney U test (implemented in R).

For all immunofluorescence experiments, we mounted ovaries with ProLong Gold Antifade Reagent with DAPI (Thermo Fisher Scientific, Waltham, MA). We imaged slides at 63x magnification on a Leica TCS SP8 Four Channel Spectral Confocal System. For each experiment, we used the same imaging parameters across genotypes and reproductive state.

Fertility assay

To further evaluate whether the LP line entered canonical diapause similarly to the temperate HP line, we assayed diapause-induced preservation of fertility in both lines. We counted progeny of females crossed to wildtype (w^{1118}) males after diapause exit at 28 days in 12°C. We compared these females to age-matched controls (maintained at 25°C for 28 days) crossed in parallel to wildtype (w^{1118}) males. In each vial, we crossed three females and six males. We replicated each cross across 12 vials and flipped each cross onto fresh food every three days. To exclude age-dependent male fertility effects, we replaced the six males every three days with one to three day old males. We recorded the number of adult progeny from each flip. We compared the mean number of progeny from diapause and age-matched control using a Mann-Whitney U test (implemented in R).

ACKNOWLEDGEMENTS

We thank the Levine Lab, A. Das, D. Dudka, E. Joyce, D. Wagner, and N. Bonini for discussions about the project and the Levine Lab and D. Wagner for feedback on the manuscript. This work was supported by Start Up funds and University Research Fund award from the University of Pennsylvania School of Arts and Sciences to M.T.L and P.S.

AUTHOR CONTRIBUTIONS

M.T.L., A.D.E., and P.S. designed the experiments. A.D.E. and R.A.F. performed the experiments. A.D.E. analyzed the experiments. M.T.L. and A.D.E. wrote the manuscript.

DECLARATION OF INTERESTS

The authors declare no competing interests.

LITERATURE CITED

1. L. S. Mills *et al.*, Camouflage mismatch in seasonal coat color due to decreased snow duration. *Proceedings of the National Acadademy of Sciences* **110**, 7360-7365 (2013).
2. N. Fielenbach, A. Antebi, C. elegans dauer formation and the molecular basis of plasticity. *Genes & Development* **22**, 2149-2165 (2008).
3. R. C. Cassada, R. L. Russell, The dauerlarva, a post-embryonic developmental variant of the nematode Caenorhabditis elegans. *Developmental Biology* **46**, 326-342 (1975).
4. C. H. Yang, J. Andrew Pospisilik, Polyphenism - A Window Into Gene-Environment Interactions and Phenotypic Plasticity. *Frontiers in Genetics* **10**, 132 (2019).
5. R. J. Sommer, Phenotypic Plasticity: From Theory and Genetics to Current and Future Challenges. *Genetics* **215**, 1-13 (2020).
6. P. Beldade, A. R. Mateus, R. A. Keller, Evolution and molecular mechanisms of adaptive developmental plasticity. *Mol Ecol* **20**, 1347-1363 (2011).
7. E. Lafuente, P. Beldade, Genomics of Developmental Plasticity in Animals. *Frontiers in Genetics* **10**, 720 (2019).

636 8. L. C. Weiss, Sensory Ecology of Predator-Induced Phenotypic Plasticity. *Frontiers in Behavioral*
637 *Neuroscience* **12**, 330 (2018).
638 9. B. M. Turner, Cellular memory and the histone code. *Cell* **111**, 285-291 (2002).
639 10. B. Papp, K. Plath, Epigenetics of reprogramming to induced pluripotency. *Cell* **152**, 1324-1343
640 (2013).
641 11. L. Ringrose, R. Paro, Polycomb/Trithorax response elements and epigenetic memory of cell
642 identity. *Development* **134**, 223-232 (2007).
643 12. N. Lee, C. Maurange, L. Ringrose, R. Paro, Suppression of Polycomb group proteins by JNK
644 signalling induces transdetermination in Drosophila imaginal discs. *Nature* **438**, 234-237 (2005).
645 13. T. Chen, S. Y. Dent, Chromatin modifiers and remodellers: regulators of cellular differentiation.
646 *Nat Rev Genet* **15**, 93-106 (2014).
647 14. Z. D. Smith, A. Meissner, DNA methylation: roles in mammalian development. *Nature Reviews*
648 *Genetics* **14**, 204-220 (2013).
649 15. P. J. Skene, S. Henikoff, Histone variants in pluripotency and disease. *Development* **140**, 2513-
650 2524 (2013).
651 16. X. Chen, M. Hiller, Y. Sancak, M. T. Fuller, Tissue-specific TAFs counteract Polycomb to turn on
652 terminal differentiation. *Science* **310**, 869-872 (2005).
653 17. L. R. Lee, D. L. Wengier, D. C. Bergmann, Cell-type-specific transcriptome and histone
654 modification dynamics during cellular reprogramming in the Arabidopsis stomatal lineage.
655 *Proceedings of the National Academy of Sciences* **116**, 21914-21924 (2019).
656 18. M. E. Valk-Lingbeek, S. W. Bruggeman, M. van Lohuizen, Stem cells and cancer; the polycomb
657 connection. *Cell* **118**, 409-418 (2004).
658 19. M. Spivakov, A. G. Fisher, Epigenetic signatures of stem-cell identity. *Nat Rev Genet* **8**, 263-271
659 (2007).
660 20. M. Ashburner, Patterns of puffing activity in the salivary gland chromosomes of Drosophila. I.
661 Autosomal puffing patterns in a laboratory stock of Drosophila melanogaster. *Chromosoma* **21**,
662 398-428 (1967).
663 21. M. Ashburner, Patterns of puffing activity in the salivary gland chromosomes of Drosophila. V.
664 Responses to environmental treatments. *Chromosoma* **31**, 356-376 (1970).
665 22. M. Berthiaume, N. Boufaied, A. Moisan, L. Gaudreau, High levels of oxidative stress globally
666 inhibit gene transcription and histone acetylation. *DNA and Cell Biology* **25**, 124-134 (2006).
667 23. H. C. Causton *et al.*, Remodeling of yeast genome expression in response to environmental
668 changes. *Molecular Biology of the Cell* **12**, 323-337 (2001).
669 24. S. R. Uffenbeck, J. E. Krebs, The role of chromatin structure in regulating stress-induced
670 transcription in Saccharomyces cerevisiae. *Biochemistry and Cell Biology* **84**, 477-489 (2006).
671 25. J. W. Gowen, E. H. Gay, Chromosome Constitution and Behavior in Eversporting and Mottling
672 in Drosophila Melanogaster. *Genetics* **19**, 189-208 (1934).
673 26. J. Zhao, J. Herrera-Diaz, D. S. Gross, Domain-wide displacement of histones by activated heat
674 shock factor occurs independently of Swi/Snf and is not correlated with RNA polymerase II
675 density. *Molecular and Cellular Biology* **25**, 8985-8999 (2005).
676 27. J. M. Kim, T. Sasaki, M. Ueda, K. Sako, M. Seki, Chromatin changes in response to drought,
677 salinity, heat, and cold stresses in plants. *Frontiers in Plant Science* **6**, 114 (2015).
678 28. H. Dai, Z. Wang, Histone Modification Patterns and Their Responses to Environment. *Current*
679 *Environmental Health Reports* **1**, 11-21 (2014).
680 29. T. Ozawa *et al.*, Histone deacetylases control module-specific phenotypic plasticity in beetle
681 weapons. *Proceedings of the National Academy of Sciences* **113**, 15042-15047 (2016).
682 30. D. F. Simola *et al.*, Epigenetic (re)programming of caste-specific behavior in the ant
683 Camponotus floridanus. *Science* **351** (2016).
684 31. C.-K. Hu *et al.*, Vertebrate diapause preserves organisms long term through Polycomb complex
685 members. *Science* **367**, 870-874 (2020).
686 32. R. Kucharski, J. Maleszka, S. Foret, R. Maleszka, Nutritional Control of Reproductive Status in
687 Honeybees via DNA Methylation. *Science* **319**, 1827-1830 (2008).

688 33. Y. X. Lu, D. L. Denlinger, W. H. Xu, Polycomb repressive complex 2 (PRC2) protein ESC
689 regulates insect developmental timing by mediating H3K27me3 and activating
690 prothoracicotropic hormone gene expression. *Journal of Biological Chemistry* **288**, 23554-23564
691 (2013).
692 34. M. Pegoraro, A. Bafna, N. J. Davies, D. M. Shuker, E. Tauber, DNA methylation changes
693 induced by long and short photoperiods in Nasonia. *Genome Research* **26**, 203-210 (2016).
694 35. D. Saunders, D. Richard, S. Applebaum, M. Ma, L. Gilbert, Photoperiodic diapause in
695 Drosophila melanogaster involves a block to the juvenile hormone regulation of ovarian
696 maturation. *General and comparative endocrinology* **79**, 174-184 (1990).
697 36. O. I. Kubrak, L. Kucerova, U. Theopold, D. R. Nassel, The Sleeping Beauty: How Reproductive
698 Diapause Affects Hormone Signaling, Metabolism, Immune Response and Somatic
699 Maintenance in Drosophila melanogaster. *Plos One* **9**, e113051 (2014).
700 37. L. Kučerová *et al.*, Slowed aging during reproductive dormancy is reflected in genome-wide
701 transcriptome changes in Drosophila melanogaster. *BMC Genomics* **17** (2016).
702 38. M. Allen, What makes a fly enter diapause? *Fly* **1**, 307-310 (2007).
703 39. V. Koštál, Eco-physiological phases of insect diapause. *Journal of Insect Physiology* **52**, 113-
704 127 (2006).
705 40. D. S. Saunders, V. C. Henrich, L. I. Gilbert, Induction of diapause in Drosophila melanogaster:
706 photoperiodic regulation and the impact of arrhythmic clock mutations on time measurement.
707 *Proceedings of the National Academy of Sciences* **86**, 3748-3752 (1989).
708 41. D. S. Saunders, L. I. Gilbert, Regulation of ovarian diapause in Drosophila melanogaster by
709 photoperiod and moderately low temperature. *Journal of Insect Physiology* **36**, 195-200 (1990).
710 42. M. Tatar, Susan A. Chien, Nicholas K. Priest, Negligible Senescence during Reproductive
711 Dormancy inDrosophila melanogaster. *The American Naturalist* **158**, 248-258 (2001).
712 43. P. S. Schmidt, L. Matzkin, M. Ippolito, W. F. Eanes, Geographic Variation in Diapause
713 Incidence, Life-History Traits, and Climatic Adaptation In drosophila Melanogaster. *Evolution* **59**,
714 1721-1732 (2005).
715 44. P. S. Schmidt, A. B. Paaby, M. S. Heschel, Genetic Variance for Diapause Expression and
716 Associated Life Histories in Drosophila Melanogaster. *Evolution* **59** (2005).
717 45. M. Tatar, C. Yin, Slow aging during insect reproductive diapause: why butterflies, grasshoppers
718 and flies are like worms. *Experimental Gerontology* **36**, 723-738 (2001).
719 46. S. Easwaran, M. Van Ligten, M. Kui, D. J. Montell, Enhanced germline stem cell longevity in
720 Drosophila diapause. *Nature Communications* **13** (2022).
721 47. M. D. Anway, A. S. Cupp, M. Uzumcu, M. K. Skinner, Epigenetic Transgenerational Actions of
722 Endocrine Disruptors and Male Fertility. *Science* **308**, 1466-1469 (2005).
723 48. R. R. Newbold, E. Padilla-Banks, W. N. Jefferson, Adverse Effects of the Model Environmental
724 Estrogen Diethylstilbestrol Are Transmitted to Subsequent Generations. *Endocrinology* **147**,
725 s11-s17 (2006).
726 49. E. E. Nilsson, M. K. Skinner, Environmentally Induced Epigenetic Transgenerational Inheritance
727 of Reproductive Disease1. *Biology of Reproduction* **93** (2015).
728 50. K. Casier, A. Boivin, C. Carré, L. Teysset, Environmentally-Induced Transgenerational
729 Epigenetic Inheritance: Implication of PIWI Interacting RNAs. *Cells* **8** (2019).
730 51. L. Houri-Ze'evi *et al.*, A Tunable Mechanism Determines the Duration of the Transgenerational
731 Small RNA Inheritance in C. elegans. *Cell* **165**, 88-99 (2016).
732 52. A. Klosin, B. Lehner, Mechanisms, timescales and principles of trans-generational epigenetic
733 inheritance in animals. *Current Opinion in Genetics & Development* **36**, 41-49 (2016).
734 53. R. Jaenisch, A. Bird, Epigenetic regulation of gene expression: how the genome integrates
735 intrinsic and environmental signals. *Nature Genetics* **33**, 245-254 (2003).
736 54. X. Zhao *et al.*, Global Transcriptional Profiling of Diapause and Climatic Adaptation in
737 Drosophila melanogaster. *Molecular Biology and Evolution* **33**, 707-720 (2016).
738 55. A. S. Quina, M. Buschbeck, L. Di Croce, Chromatin structure and epigenetics. *Biochemical*
739 *Pharmacology* **72**, 1563-1569 (2006).

740 56. P. Oudet, M. Gross-Bellard, P. Chambon, Electron microscopic and biochemical evidence that
741 chromatin structure is a repeating unit. *Cell* **4**, 281-300 (1975).
742 57. T. Kouzarides, Chromatin Modifications and Their Function. *Cell* **128**, 693-705 (2007).
743 58. M. Lawrence, S. Daujat, R. Schneider, Lateral Thinking: How Histone Modifications Regulate
744 Gene Expression. *Trends in Genetics* **32**, 42-56 (2016).
745 59. T. Zhang, S. Cooper, N. Brockdorff, The interplay of histone modifications - writers that read.
746 *EMBO Rep* **16**, 1467-1481 (2015).
747 60. K. D. Williams, M. B. Sokolowski, Diapause in Drosophila melanogaster females: a genetic
748 analysis. *Heredity* **71**, 312-317 (1993).
749 61. K. J. Emerson *et al.*, Environmental control of ovarian dormancy in natural populations of
750 Drosophila melanogaster. *J Comp Physiol A Neuroethol Sens Neural Behav Physiol* **195**, 825-
751 829 (2009).
752 62. K. J. Emerson *et al.*, Environmental control of ovarian dormancy in natural populations of
753 Drosophila melanogaster. *Journal of Comparative Physiology A* **195**, 825-829 (2009).
754 63. M. Lirakis, M. Dolezal, C. Schlötterer, Redefining reproductive dormancy in Drosophila as a
755 general stress response to cold temperatures. *Journal of Insect Physiology* **107**, 175-185
756 (2018).
757 64. P. J. Skene, S. Henikoff, An efficient targeted nuclease strategy for high-resolution mapping of
758 DNA binding sites. *eLife* **6** (2017).
759 65. F. Lyko, B. H. Ramsahoye, R. Jaenisch, DNA methylation in Drosophila melanogaster. *Nature*
760 **408**, 538-540 (2000).
761 66. Lauren N. Booth, A. Brunet, The Aging Epigenome. *Molecular Cell* **62**, 728-744 (2016).
762 67. L. Li, C. Greer, R. N. Eisenman, J. Secombe, Essential functions of the histone demethylase lid.
763 *PLoS Genet* **6**, e1001221 (2010).
764 68. I. J. Chamani, D. L. Keefe, Epigenetics and Female Reproductive Aging. *Frontiers in*
765 *Endocrinology* **10** (2019).
766 69. S. Pal, J. K. Tyler, Epigenetics and aging. *Science Advances* **2** (2016).
767 70. P. D. Kaufman, O. J. Rando, Chromatin as a potential carrier of heritable information. *Current*
768 *Opinion in Cell Biology* **22**, 284-290 (2010).
769 71. P. Sarkies, Molecular mechanisms of epigenetic inheritance: Possible evolutionary implications.
770 *Seminars in Cell & Developmental Biology* **97**, 106-115 (2020).
771 72. J. A. Reynolds, J. Clark, S. J. Diakoff, D. L. Denlinger, Transcriptional evidence for small RNA
772 regulation of pupal diapause in the flesh fly, Sarcophaga bullata. *Insect Biochem Mol Biol* **43**,
773 982-989 (2013).
774 73. A. K. Webster, J. M. Jordan, J. D. Hibshman, R. Chitrakar, L. R. Baugh, Transgenerational
775 Effects of Extended Dauer Diapause on Starvation Survival and Gene Expression Plasticity in
776 Caenorhabditis elegans. *Genetics* **210**, 263-274 (2018).
777 74. C. C. Phillis *et al.*, Shifting Thresholds: Rapid Evolution of Migratory Life Histories in
778 Steelhead/Rainbow Trout,Oncorhynchus mykiss. *Journal of Heredity* **107**, 51-60 (2016).
779 75. B. W. Robinson, D. S. Wilson, Genetic variation and phenotypic plasticity in a trophically
780 polymorphic population of pumpkinseed sunfish (Lepomis gibbosus). *Evolutionary Ecology* **10**,
781 631-652 (1996).
782 76. B. J. Parker, R. M. H. Driscoll, M. E. Grantham, J. Hrcek, J. A. Brisson, Wing plasticity and
783 associated gene expression varies across the pea aphid biotype complex. *Evolution* **75**, 1143-
784 1149 (2021).
785 77. T. E. Reddy *et al.*, Methylation QTLs Are Associated with Coordinated Changes in Transcription
786 Factor Binding, Histone Modifications, and Gene Expression Levels. *PLoS Genetics* **10** (2014).
787 78. Y. Zhang, J. M. Wendte, L. Ji, R. J. Schmitz, Natural variation in DNA methylation homeostasis
788 and the emergence of epialleles. *Proceedings of the National Academy of Sciences* **117**, 4874-
789 4884 (2020).

79. S. R. Eichten, M. W. Vaughn, P. J. Hermanson, N. M. Springer, Variation in DNA Methylation Patterns is More Common among Maize Inbreds than among Tissues. *The Plant Genome* **6** (2013).
80. C. Rintisch *et al.*, Natural variation of histone modification and its impact on gene expression in the rat genome. *Genome Research* **24**, 942-953 (2014).
81. M. Yang *et al.*, Natural variation of H3K27me3 modification in two Arabidopsis accessions and their hybrid. *Journal of Integrative Plant Biology* **58**, 466-474 (2015).
82. J. J. Herman, S. E. Sultan, DNA methylation mediates genetic variation for adaptive transgenerational plasticity. *Proceedings of the Royal Society B: Biological Sciences* **283** (2016).
83. P. S. Schmidt, D. R. Conde, Environmental heterogeneity and the maintenance of genetic variation for reproductive diapause in Drosophila melanogaster. *Evolution* **60**, 1602-1611 (2006).
84. H. E. Machado *et al.*, Comparative population genomics of latitudinal variation in Drosophila simulans and Drosophila melanogaster. *Molecular Ecology* **25**, 723-740 (2016).
85. M. T. Levine, D. J. Begun, Evidence of Spatially Varying Selection Acting on Four Chromatin-Remodeling Loci in Drosophila melanogaster. *Genetics* **179**, 475-485 (2008).
86. J. A. Reinhardt, B. Kolaczkowski, C. D. Jones, D. J. Begun, A. D. Kern, Parallel Geographic Variation in Drosophila melanogaster. *Genetics* **197**, 361-373 (2014).
87. D. J. Wuebbles *et al.*, Climate Science Special Report: Fourth National Climate Assessment. *U.S. Global Change Research Program* **1** (2017).
88. R. C. King, *Ovarian development in Drosophila melanogaster* (Academic Press, New York, 1970).
89. B. Edgar *et al.*, Bellymount enables longitudinal, intravital imaging of abdominal organs and the gut microbiota in adult Drosophila. *PLOS Biology* **18** (2020).
90. A. M. Bolger, M. Lohse, B. Usadel, Trimmomatic: a flexible trimmer for Illumina sequence data. *Bioinformatics* **30**, 2114-2120 (2014).
91. A. Dobin *et al.*, STAR: ultrafast universal RNA-seq aligner. *Bioinformatics* **29**, 15-21 (2013).
92. Y. Liao, G. K. Smyth, W. Shi, featureCounts: an efficient general purpose program for assigning sequence reads to genomic features. *Bioinformatics* **30**, 923-930 (2013).
93. M. I. Love, W. Huber, S. Anders, Moderated estimation of fold change and dispersion for RNA-seq data with DESeq2. *Genome Biology* **15** (2014).
94. T. L. Orr-Weaver, Drosophila chorion genes: Cracking the eggshell's secrets. *BioEssays* **13**, 97-105 (1991).
95. M. Gillespie *et al.*, The reactome pathway knowledgebase 2022. *Nucleic Acids Research* **50**, D687-D692 (2022).
96. S. Stael, L. P. Miller, Á. D. Fernández-Fernández, F. Van Breusegem, "Detection of Damage-Activated Metacaspase Activity by Western Blot in Plants" in Plant Proteases and Plant Cell Death. (2022), 10.1007/978-1-0716-2079-3_11 chap. Chapter 11, pp. 127-137.
97. L. A. Perkins *et al.*, The Transgenic RNAi Project at Harvard Medical School: Resources and Validation. *Genetics* **201**, 843-852 (2015).
98. L. N. Petrella, T. Smith-Leiker, L. Cooley, The Ovhts polyprotein is cleaved to produce fusome and ring canal proteins required forDrosophilaoogenesis. *Development* **134**, 703-712 (2007).
99. R. Camato, R. M. Tanguay, Changes in the methylation pattern of core histones during heat-shock in Drosophila cells. *The EMBO Journal* **1**, 1529-1532 (1982).
100. A. Fellous, P. Favrel, G. Riviere, Temperature influences histone methylation and mRNA expression of the Jmj-C histone-demethylase orthologues during the early development of the oyster Crassostrea gigas. *Marine Genomics* **19**, 23-30 (2015).
101. G. Szittya, Low temperature inhibits RNA silencing-mediated defence by the control of siRNA generation. *The EMBO Journal* **22**, 633-640 (2003).
102. A. H. Brand, A. S. Manoukian, N. Perrimon, "Chapter 33 Ectopic Expression in Drosophila" in Methods in Cell Biology. (1994), 10.1016/s0091-679x(08)60936-x, pp. 635-654.

842 103. K. S. McKim, E. F. Joyce, J. K. Jang, "Cytological Analysis of Meiosis in Fixed Drosophila
843 Ovaries" in Meiosis. (2009), 10.1007/978-1-60761-103-5_12 chap. Chapter 12, pp. 197-216.
844 104. T. Xie, A. C. Spradling, A Niche Maintaining Germ Line Stem Cells in the DrosophilaOvary.
845 *Science* **290**, 328-330 (2000).
846 105. J. Schindelin *et al.*, Fiji: an open-source platform for biological-image analysis. *Nature Methods*
847 **9**, 676-682 (2012).

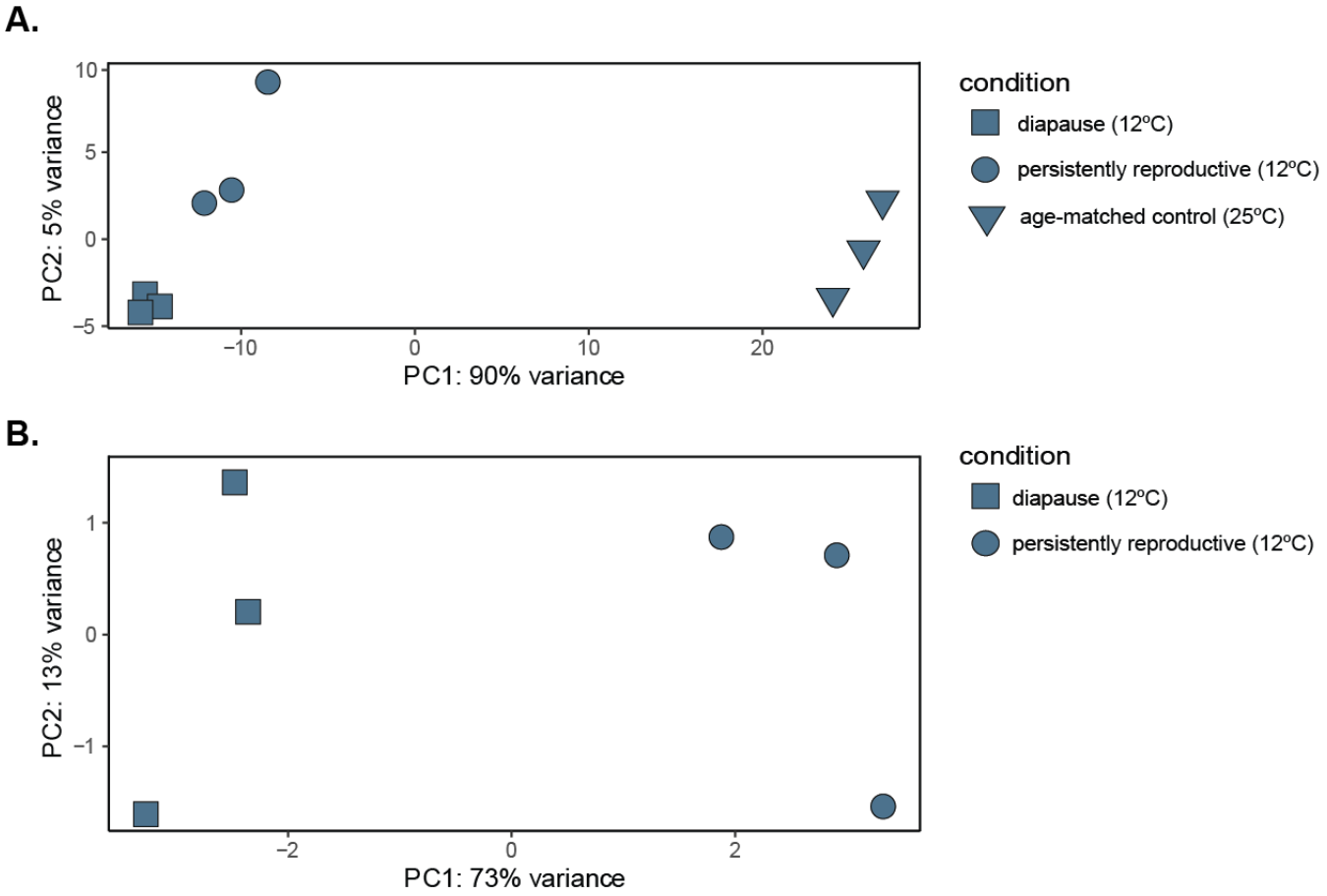

Evans et al. Figure S1

Figure S1. Principal component analysis (PCA) of RNA-seq from the temperate North American inbred line. (A) PCA of RNA-seq reads from diapausing (square), persistently reproductive (circle), and age-matched control (triangle) ovaries, stages 1-7 only. Note that temperature explains most of the variance between the three samples (PC1, 90%). (B) PCA of RNA-seq reads from diapausing and persistently reproductive ovaries only.

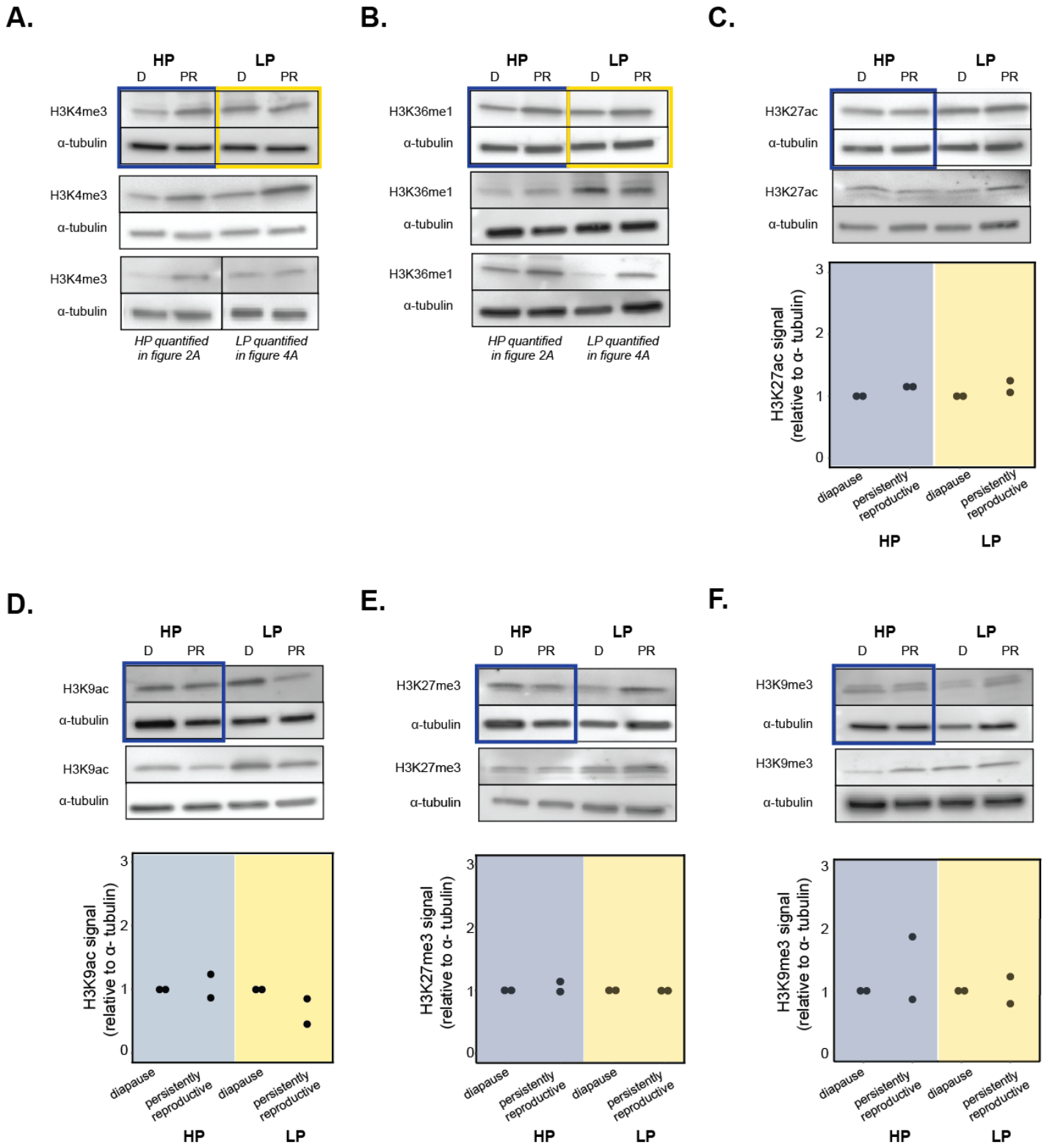

Evans et al. Figure S2

853 **Figure S2. Western blots probed for various histone marks on multiple biological replicates.**
854 Blots of ovary lysate prepared from diapausing and persistently reproductive ovaries and quantification
855 relative to α-tubulin loading control of (A) H3K4me3, (B) H3K36me1, (C) H3K27ac, (D) H3K9ac, (E)
856 H3K27me3, and (F) H3K9me3. Blue boxes delineate replicates shown in Fig. 2A, yellow boxes
857 delineate replicates shown in Fig. 4A. D = diapause, PR = persistently reproductive.

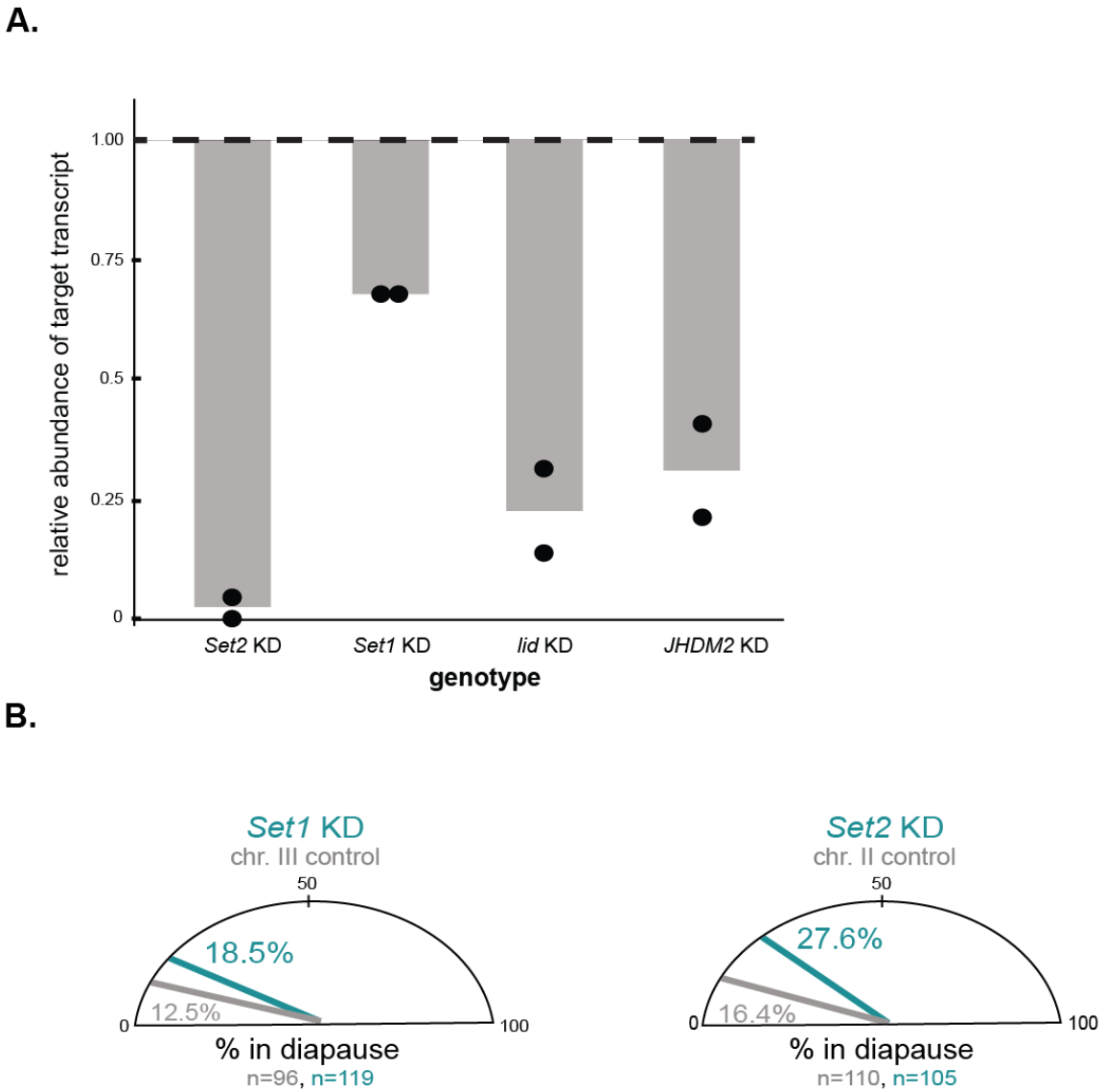

Evans et al. Figure S3

Figure S3. Quality control of RNAi experiments. (A) RT-qPCR confirming knockdown (KD) of transcripts targeted by RNAi. Note *Set2* and *lid* knockdown genotypes are compared to chromosome II control genotype, while *Set1* and *JHDM2* knockdown genotypes are compared to chromosome III control genotype. (B) Diapause plasticity of daughters, whose mothers underwent diapause, with *Set1* or *Set2* knocked down in the ovary. The abundance of persistently reproductive ovaries in both genotypes verified that knockdown of *Set1* or *Set2* alone, at 12°C, does not block ovary development (see Methods). “chr.” = chromosome.

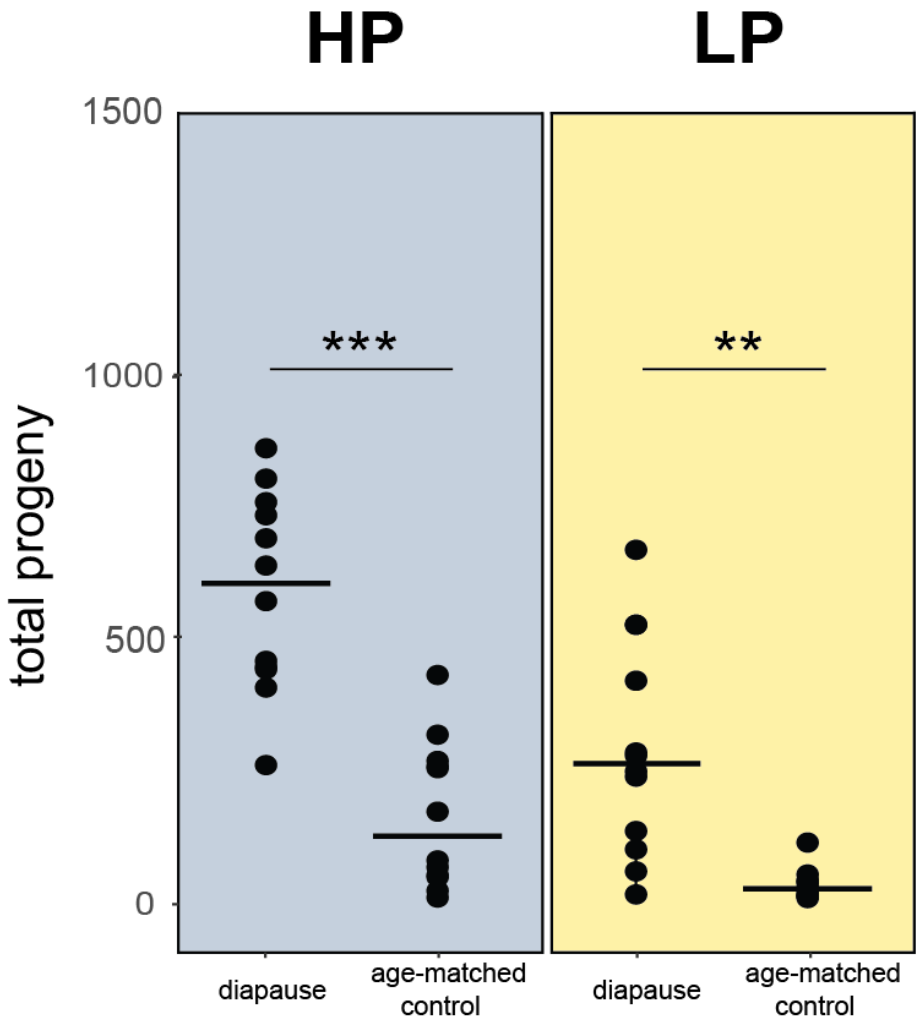

Evans et al. Figure S4

Figure S4. Total progeny from diapause and age-matched control females of the HP line (blue) and LP line (yellow). Each replicate represents a vial of three females. t-test, *** $p<0.001$, ** $p<0.01$

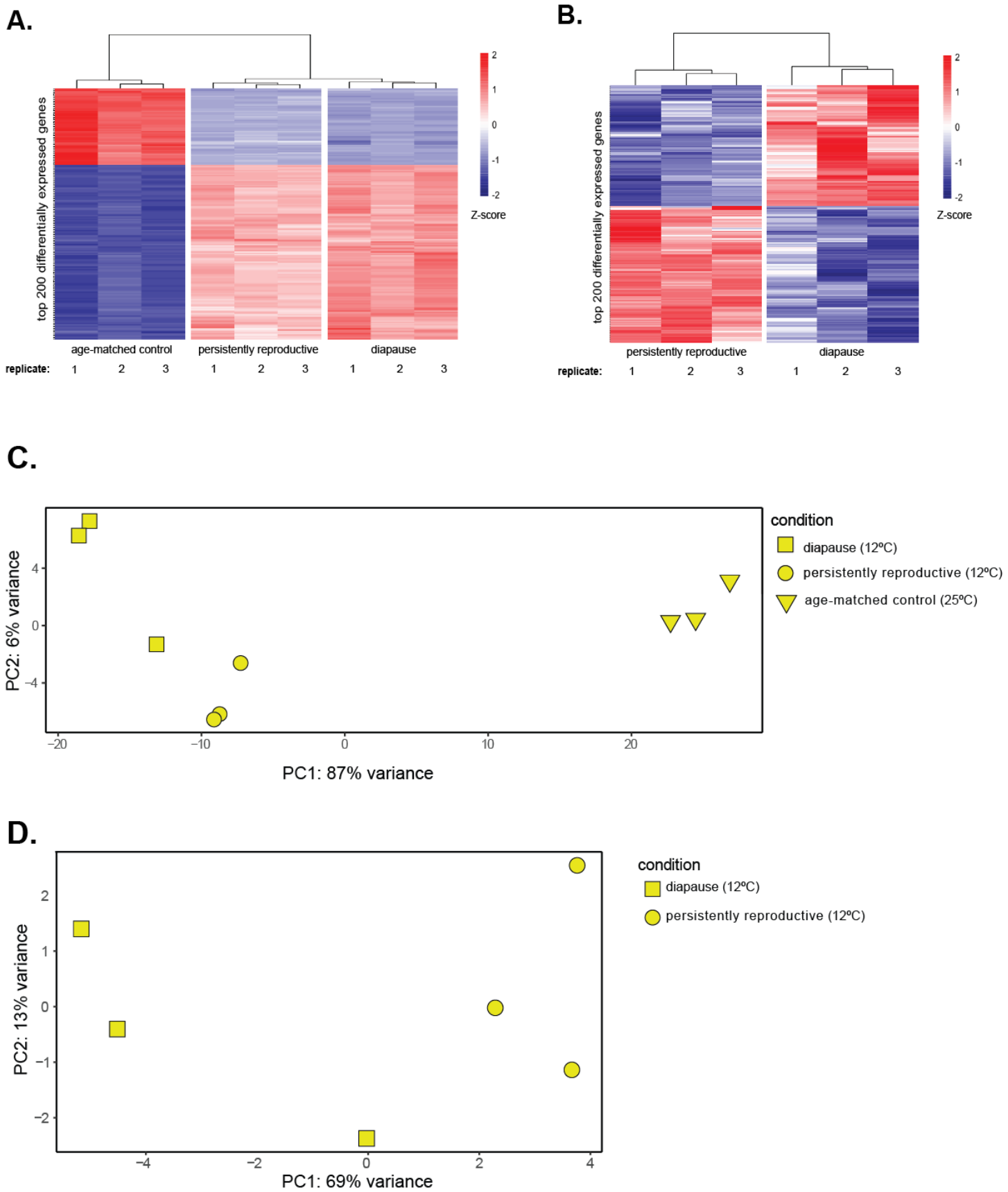

Evans et al. Figure S5

872 **Figure S5. Analysis of the LP line ovary RNA-seq.** (A) Heatmap of the top 200 significantly
873 differentially expressed genes (by FDR) between age-matched control, diapausing, and persistently
874 reproductive ovaries, stages 1-7 only. Blue-red gradient depicts the Z-score of each gene. Red
875 corresponds to upregulated genes and blue corresponds to downregulated genes. (B) Heatmap of the
876 top 200 significantly differentially expressed genes (by FDR) between diapausing and persistently
877 reproductive ovaries only. Blue-red gradient depicts the Z-score of each gene. Red corresponds to
878 upregulated genes and blue corresponds to downregulated genes. (C) PCA of RNA-seq reads from
879 diapausing (square), persistently reproductive (circle), and age-matched control (triangle) ovaries. Note
880 that temperature explains most of the variance among the three samples (PC1, 87%). (D) PCA of RNA-
881 seq reads from diapausing and persistently reproductive ovaries.

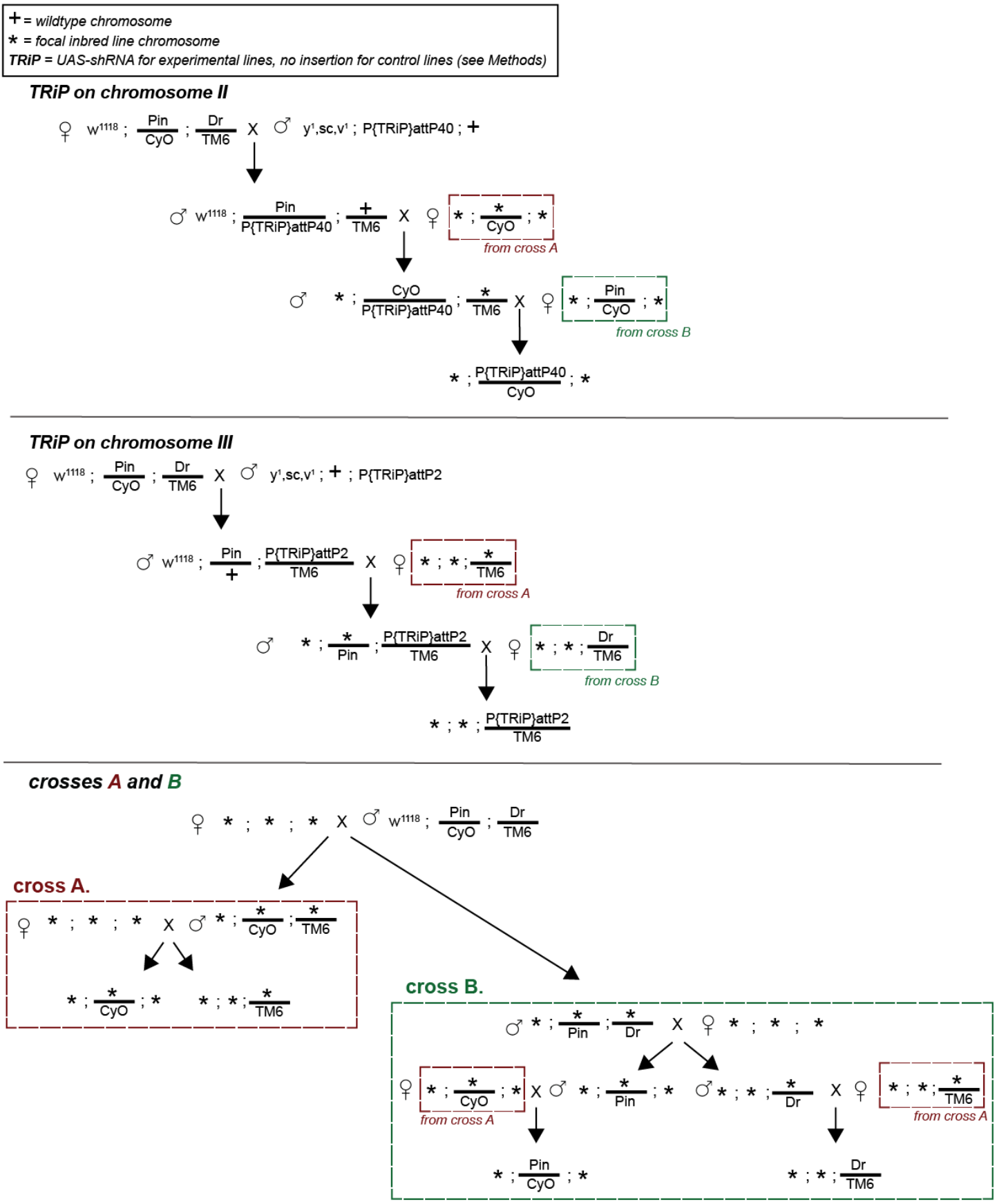

Evans et al. Figure S6

882 **Figure S6. Crossing scheme used to generate transcript knockdown and control lines.** Brown
883 dashed boxes correspond to lines constructed from cross A (bottom) and green dashed boxes
884 correspond to lines constructed from cross B (bottom).

885 SUPPLEMENTARY TABLE LEGEND
886
887 **Table S1. Primers used in study.**
888

Forward	Reverse	Purpose
TTTGCCTTCCTGTTTTTGCT	ATAATACCGCGCCACATAGC	Amplifies the AmpR gene to screen for the introduction of TRiP chromosomes
TAATGCTGCGGCCGTTGAGG	CGAACAACTCTAGCTCCTCC	RT-qPCR primer for *lid* transcription [1]
GTTTTCAGTGCATGACCAAG	GGCAACGAGCTCTAGTGATG	RT-qPCR primer for *JHDM2* transcription [2]
CGTTCGGAATATCAACCTGGTC	GTAACGATAGAGTCTGGTACCAC	RT-qPCR primer for *Set1* transcription [3]
ACGGGTGGCTAATATGGAGA	TTCTTCTCCGTGCGAAAAAC	RT-qPCR primer for *Set2* transcription [4]
ATGACCATCCGCCCAGCATAC	GTTCTGCATGAGCAGGACCTCC	RT-qPCR primer for *RP49* transcription (housekeeping gene)

889
890 SUPPLEMENTARY REFERENCES
891

892 1. Drelon, C., H.M. Belalcazar, and J. Secombe, *The Histone Demethylase KDM5 Is Essential for*
893 *Larval Growth in Drosophila.* Genetics, 2018. **209**(3): p. 773-787.
894 2. Lorbeck, M.T., N. Singh, A. Zervos, M. Dhatta, M. Lapchenko*, et al.*, *The histone demethylase*
895 *Dmel\Kdm4A controls genes required for life span and male-specific sex determination in*
896 *Drosophila.* Gene, 2010. **450**(1-2): p. 8-17.
897 3. Hallson, G., R.E. Hollebakken, T. Li, M. Syrzycka, I. Kim*, et al.*, *dSet1 Is the Main H3K4 Di- and*
898 *Tri-Methyltransferase Throughout Drosophila Development.* Genetics, 2012. **190**(1): p. 91-100.
899 4. Stabell, M., J. Larsson, R.B. Aalen, and A. Lambertsson, *Drosophila dSet2 functions in H3-K36*
900 *methylation and is required for development.* Biochemical and Biophysical